Non-Ionic Amphiphilic Homopolymers: Synthesis, Solution Properties, and Biochemical Validation

ARTICLE *in* LANGMUIR · FEBRUARY 2012

Impact Factor: 4.46 · DOI: 10.1021/la205026r · Source: PubMed

10 AUTHORS, INCLUDING:

Grégory Durand
Université d´Avignon et des Pays du Vaucluse
56 PUBLICATIONS **713** CITATIONS
SEE PROFILE

Paola Bazzacco
11 PUBLICATIONS **292** CITATIONS
SEE PROFILE

Emmanuelle Billon-Denis
Armed Forces Biomedical Research Institute, …
11 PUBLICATIONS **239** CITATIONS
SEE PROFILE

Christine Ebel
French National Centre for Scientific Research
136 PUBLICATIONS **3,486** CITATIONS
SEE PROFILE

Langmuir

Article

pubs.acs.org/Langmuir

Non-Ionic Amphiphilic Homopolymers: Synthesis, Solution Properties, and Biochemical Validation

K. Shivaji Sharma,[†,¶] Grégory Durand,[*,†,‡] Frank Gabel,[§,∥,⊥] Paola Bazzacco,[#] Christel Le Bon,[#] Emmanuelle Billon-Denis,[#] Laurent J. Catoire,[#] Jean-Luc Popot,[*,#] Christine Ebel,[*,§,∥,⊥] and Bernard Pucci[†,‡]

[†]Université d'Avignon et des Pays de Vaucluse, Equipe Chimie Bioorganique et Systèmes Amphiphiles, 33 rue Louis Pasteur, F-84000 Avignon, France

[‡]Unité Mixte de Recherche 5247, Centre National de la Recherche Scientifique and Universités de Montpellier 1&2, Institut des Biomolécules Max Mousseron, Faculté de Pharmacie, 15 avenue Charles Flahault, F-34093 Montpellier Cedex 05, France

[§]CEA, Institut de Biologie Structurale Jean-Pierre Ebel, 41 rue Jules Horowitz, F-38027, Grenoble, France

[∥]CNRS, Institut de Biologie Structurale Jean-Pierre Ebel, Grenoble, France

[⊥]Université Joseph Fourier − Grenoble 1, Institut de Biologie Structurale Jean-Pierre Ebel, Grenoble, France

[#]Unité Mixte de Recherche 7099, Centre National de la Recherche Scientifique and Université Paris 7, Institut de Biologie Physico-Chimique, 13 rue Pierre-et-Marie Curie, F-75005 Paris, France

Supporting Information

ABSTRACT: A novel type of nonionic amphipols for handling membrane proteins in detergent-free aqueous solutions has been obtained through free-radical homo-telomerization of an acrylamide-based monomer comprising a C_{11} alkyl chain and two glucose moieties, using a thiol as transfer reagent. By controlling the thiol/monomer ratio, the number-average molecular weight of the polymers was varied from 8 to 63 kDa. Homopolymeric nonionic amphipols were found to be highly soluble in water and to self-organize, within a large concentration range, into small, compact particles of ∼6 nm diameter with a narrow size distribution, regardless of the molecular weight of the polymer. They proved able to trap and stabilize two test membrane proteins, bacteriorhodopsin from *Halobium salinarum* and the outer membrane protein X of *Escherichia coli*, under the form of small and well-defined complexes, whose size, composition, and shape were studied by aqueous size-exclusion chromatography, analytical ultracentrifugation, and small-angle neutron scattering. As shown in a companion paper, nonionic amphipols can be used for membrane protein folding, cell-free synthesis, and solution NMR studies (Bazzacco et al. **2012**, *Biochemistry*, DOI: 10.1021/bi201862v).

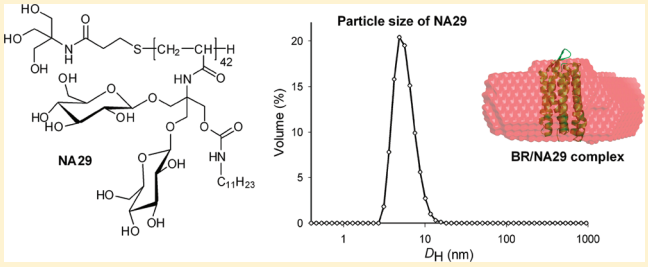

INTRODUCTION

Amphiphilic molecules self-assemble in aqueous solvents because of the differential solvation properties of their hydrophilic and lipophilic groups. In water, detergents, a class of small surfactants, form micelles that can solubilize amphiphilic and lipophilic guest molecules. This property has proven highly useful in the study of membrane proteins (MPs), which are naturally water-insoluble due to the high hydrophobicity of their transmembrane surface.[1] However, the dissociating character of detergents, combined with the need to maintain an excess of them, tends to inactivate membrane proteins. This has prompted the development of milder surfactants, such as detergents with less disruptive structures, fluorinated surfactants, lipopeptides, or nanodiscs (for reviews, see refs 2−4). A particularly promising approach consists in generating multiple contacts between an amphiphilic polymer and the hydrophobic transmembrane surface of MPs, leading to the development of the so-called 'amphipols' (APols).[5] APols have proven very efficient at keeping MPs soluble in the absence of detergents, while stabilizing them biochemically. Their applications extend to MP folding, immobilization, structural studies by solution NMR and cryo-electron microscopy, and studies of ligand binding and the recruitment of effectors, as well as vaccination (reviewed in refs 4, 6, 7). The most extensively studied APol to date, A8−35, is an anionic polymer made of poly(acrylic acid) carrying multiple octyl chains.[5] Because its solubility depends on the carboxylate groups being charged, A8−35 suffers from certain limitations, among which are its insolubility in acidic buffers[8,9] and its sensitivity to calcium ions.[10] In addition, its charged character prevents the separation of MP/A8−35

Received: December 20, 2011
Revised: February 2, 2012
Published: February 2, 2012

Scheme 1. Synthetic Strategy for the Preparation of Non-Ionic Amphipols[a]

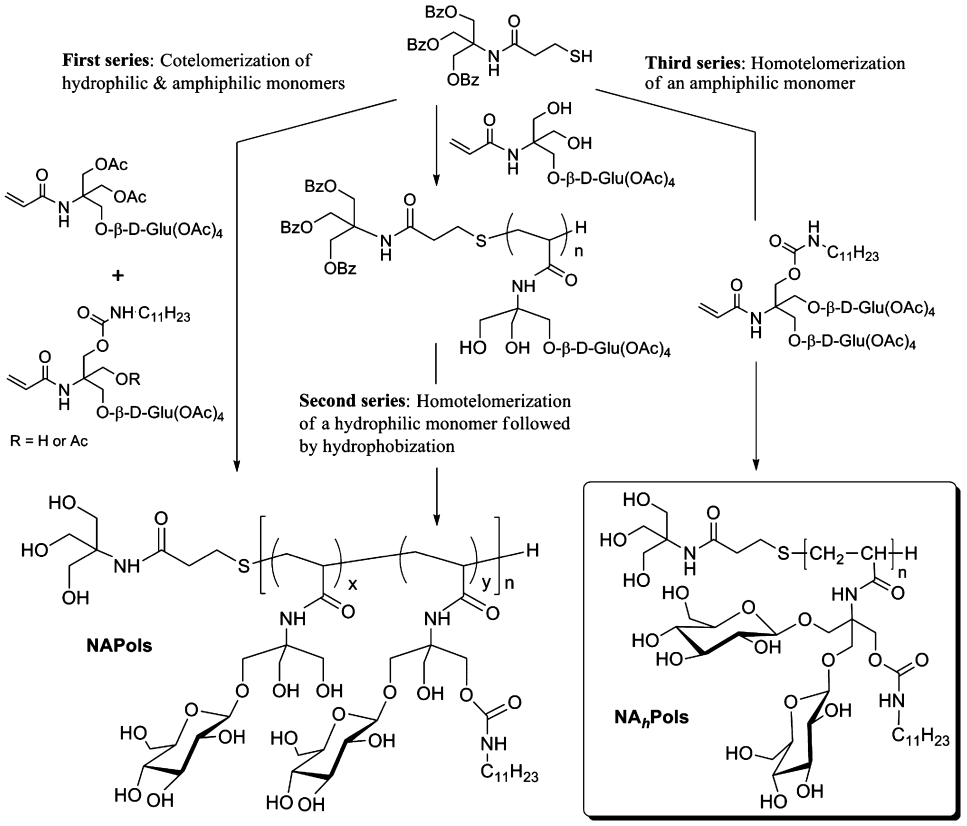

[a]Left, co-telomers.[15] Center, hydrophilic homo-telomers randomly grafted with hydrophobic chains.[16] Right, amphiphilic homo-telomers (present work).

complexes by such techniques as ion exchange chromatography or isoelectric focusing. These constraints have prompted the development of alternative, chemically different APols, including zwitterionic APols,[11,12] sulfonated APols (SAPols),[13] and nonionic amphipols (NAPols).[14−16]

The first NAPols to be synthesized and validated were short copolymers obtained by radical co-telomerization of hydrophilic and lipophilic monomers derived from *tris*(hydroxymethyl)-acrylamidomethane (THAM), in the presence of a transfer reagent. The water solubility of these polymers was rather poor, which limited their usefulness in biochemistry, but some of them were shown to be able to keep model MPs water-soluble and in their native state in the absence of detergents, providing a first proof of principle.[14] More recently, the properties of glucose-based NAPols have been investigated. Two series of heteropolymers were generated, one by co-telomerization of hydrophilic and amphiphilic glucose-based monomers,[15] the other by homo-telomerization of a hydrophilic glucose-based monomer followed by hydrophobization of the resulting homopolymer,[16] yielding similar structures by very different routes (Scheme 1, left and center). The resulting polymers feature high water-solubility and surface activity, as well as the ability to self-organize into small and compact particles of well-defined size and to trap MPs and keep them water-soluble.[16] However, none of the two synthetic routes allowed the preparation of large quantities of NAPols with high batch-to-batch reproducibility, a requirement for carrying out extended biochemical and biophysical investigations. The present article describes the development of a simpler and more convenient synthetic route to amphiphilic polymers with related structures and validates them as efficient APols.

Molecular designs based on amphiphilic homopolymers in which both hydrophilic and hydrophobic moieties are incorporated within the same monomer unit have been recently developed, leading to polymers with unique self-assembling properties and applications such as separation, catalysis, and sensing.[17−19] In the present work, we describe the synthesis and properties of nonionic homopolymeric amphipols (NA$_h$Pols), in which each repeat unit is by itself an amphiphile (Scheme 1, right). NA$_h$Pols were obtained by free-radical telomerization, in the presence of a transfer reagent, of an acrylamide-based monomer comprising a C_{11} alkyl chain and two glucose moieties.[20] The aqueous behavior of NA$_h$Pols was studied by surface tension measurements, dynamic light scattering (DLS), aqueous size exclusion chromatography (ASEC), analytical ultracentrifugation (AUC), and small-angle neutron scattering (SANS). Their potential for stabilizing MPs in aqueous solutions was studied using two model MPs, one whose transmembrane domain comprises seven α-helices and the cofactor retinal, bacteriorhodopsin (BR) from *Halobium salinarum*, and one that is made up of an eight-strand transmembrane β-barrel, *Escherichia coli*'s outer membrane protein X (OmpX). We show that NA$_h$Pols trap and stabilize both proteins in the form of small, well-defined complexes − thus offering the first example of homopolymeric APols. Perspectives for the applications of NA$_h$Pols in MP biochemistry and biophysics are discussed.

dx.doi.org/10.1021/la205026r | *Langmuir* 2012, 28, 4625−4639

MATERIALS AND METHODS

Materials, general procedures and instrumentation for the synthesis are given in the Supporting Information.

Synthesis of NA$_h$Pols (Scheme 2). The general procedure taking NA-29 as an example is as follows. The letters NA stand for "nonionic amphiphilic homopolymer", followed by the number-average molecular weight expressed in kDa. Thus, "NA29" denotes a NA$_h$Pol with a number-average molecular weight $\bar{M}_n \approx 29$ kDa. Protected monomer *p*M[20] (1.0 g, 0.97 mmol, 40.0 equiv) was dissolved in THF (15 mL). The solution was degassed by bubbling with argon for 20 min and then heated to reflux still under argon bubbling. The transfer reagent **TR**[15] (12.62 mg, 0.024 mmol, 1.0 equiv) and AIBN (1.98 mg, 0.012 mmol, 0.5 equiv) dissolved in THF (1 mL) were then simultaneously added through a microsyringe. The reaction mixture was stirred at reflux until complete consumption of protected monomer (~18 h). The reaction mixture was concentrated under vacuum, and the crude polymer was purified by gravity size-exclusion chromatography on Sephadex LH-20 resin eluting with a 1:1 (v/v) MeOH/CH_2Cl_2 mixture. The solvent was evaporated under vacuum to give the protected NA$_h$Pol as a white powder (0.524 g, 52%). Four sets of the above reaction were run and combined to give 2.07 g of NA$_h$Pol with an average 51% yield on the four reactions. ^{1}H NMR (250 MHz, $CDCl_3$) δ (ppm) 8.1–7.4 (m, C_6H_5 from **TR**), 6.6 (m, –N*H*), 5.3–4.8 (glucose unit: *H*4, *H*2, *H*3), 4.6–3.6 (glucose unit: *H*1, *H*6, *H*6′, *H*5, $-CH_2-$O), 3.1 (m, –NH–CH_2), 2.4–2.1 (bs, $-OCOCH_3$), 1.9–1.3 (CH_2-CH of the polymer chain, CH_2 of the alkyl chain), 0.8 (t, CH_3 of the alkyl chain).

Polymer Analysis. The number-average molecular weight $\bar{M}_n$ and number-average degree of polymerization $\overline{DP}_n$ of protected NA$_h$Pols were determined by UV absorbance.[15,16] The three benzoyl groups of the transfer reagent (**TR**) strongly absorb at λ = 272 nm (molar absorptivity coefficient $\varepsilon_{272} = 2.8 \times 10^3$ L.mol^{-1}.cm^{-1}). A calibration curve of the absorbance vs. the molar concentration of **TR** was first established using standard solutions at 10–580 μM in CH_2Cl_2/MeOH (1:1 v/v). A precise weight of protected NA$_h$Pol (p-NA$_h$Pol) was dissolved in CH_2Cl_2/MeOH, defining the weight concentration of polymer in g·L^{-1}. The value of the UV absorbance provided the molar concentration of the transfer reagent [**TR**] (mol.L^{-1}) in the solution. $\bar{M}_n$ was then calculated by the following equation:

$$\bar{M}_n = [\text{p-NA}_h\text{Pols}]/[\mathbf{TR}] \quad (1)$$

The $\overline{DP}_n$ of the protected NA$_h$Pol was determined through the following equation:

$$\bar{M}_n = M_{\mathbf{TR}} + [(M_{p\mathbf{M}}) \times n] \quad (2)$$

where $M_{\mathbf{TR}}$ is the molecular mass of the transfer reagent ($M_{\mathbf{TR}}$ = 522 g·mol^{-1}), $M_{p\mathbf{M}}$ that of protected monomer p**M** ($M_{p\mathbf{M}}$ = 1032 g·mol^{-1}), and n the total number of monomers. The number-average degree of polymerization $\overline{DP}_n$ is then obtained as

$$\overline{DP}_n = n + 1 \quad (3)$$

The number-average molecular weight of protected NA$_h$Pol was also obtained by ^{1}H NMR calibration, by comparing the integral area of protons from the phenyl groups at 7.4–8.1 ppm with those of the NH vicinal methylene of each protected monomer constituting the polymer backbone.

Deprotection of NA$_h$Pol. Protected NA$_h$Pol (2.0 g, 1.91 mmol) was dissolved in dry methanol (50 mL) under argon atmosphere. A catalytic amount of sodium methoxide was added and the mixture was stirred overnight at room temperature. The reaction solution was neutralized by addition of a spatula of acidic resin (IRC 50) (~pH 8) and the solution was shaken for 15 min. The solution was filtered off, and then concentrated under vacuum. The crude polymer was dissolved in methanol (20 mL) and precipitated into cold ether (250 mL). The precipitate was filtered off and the solvent was evaporated under vacuum. Finally, the resulting NA$_h$Pol was solubilized in Milli-Q water at 10 g·L^{-1}, filtered through a 0.45 μm PVDF syringe filter, and then subjected to dialysis against Milli-Q water for 24 h under continuous stirring using dialysis membrane tubing (MWCO 6–8 kDa). The resulting dialyzed solution was freeze-dried to give the NA$_h$Pol NA29 as a white powder (1.02 g, 78%). ^{1}H NMR (250 MHz, DMSO-d_6) δ (ppm) 7.1 (m, –N*H*), 5.2–4.8 (glucose unit), 4.6–3.4 (glucose unit, $-CH_2-$O), 3.2 (m, –NH–CH_2), 1.9–1.2 (CH_2-CH of the polymer chain, CH_2 of the alkyl chain), 0.8 (t, $-CH_3$ of the alkyl chain).

Deprotection of Monomer *p*M. The synthetic route was essentially the same as for the deprotection of NA$_h$Pol. The reaction solution was neutralized by addition of a spatula of acidic resin (IRC 50) (~pH 8) and the solution was shaken for 15 min. The resulting deprotected monomer *d***M** was solubilized in Milli-Q water and the solution was filtered through a 0.45 μm filter and subsequently freeze-dried to give the deprotected monomer *N*-1,1-di[(*O*-β-D-glucopyranosyl)oxymethyl]-1-[(undecylcarbamoyloxymethyl)-methyl)]-acrylamide as a white powder in quantitative yield. ^{1}H NMR (250 MHz, DMSO-d_6) δ (ppm) 7.58 (s, 1H), 7.14 (t, J = 5.7 Hz, 1H), 6.33 (dd, J = 11.0 and 16.8 Hz, 1H), 6.05 (dd, J = 2.2 and 16.8 Hz, 1H), 5.64 (d, J = 11.0 Hz, 1H), 5.2–4.8 (m, 6H), 4.6–2.8 (m, 24H), 1.5–1.1 (m, 18H), 0.87 (t, J = 6.5 Hz, 3H). ^{13}C NMR (66.86 MHz, CD_3OD) δ (ppm) 166.8, 157.4 (CO), 131.3 (CH), 125.7 (CH_2), 103.5, 103.4, 76.6, 73.6, 70.1 (CH), 67.8, 67.7, 61.4 (CH_2), 59.5 (C) 40.5, 31.7, 29.5, 29.3, 29.1, 26.5, 22.3 (CH_2), 14.5 (CH_3). HRMS (ESI+) calculated for $C_{31}H_{57}N_2O_{15}$ ([M + H]$^+$) 697.3759, found 697.3748.

Surface Tension Measurements. The surface activity of NA$_h$Pols and deprotected monomer *d***M** in solution at the air–water interface was determined by the Wilhelmy plate technique using a Krüss K-100 (Krüss, Germany) tensiometer at 22 ± 1 °C. The polymer solution was prepared 12–24 h prior to measurement using Milli-Q water. Twenty milliliters of polymer solution were taken in a glass trough and the surface tension was determined by dilution. Other conditions were as reported elsewhere.[21]

Dynamic Light Scattering. The hydrodynamic particle size distribution and polydispersity of NA$_h$Pols and deprotected monomer

Scheme 2. Synthetic Pathway for Non-Ionic Amphiphilic Homopolymers (NA$_h$Pols)[c]

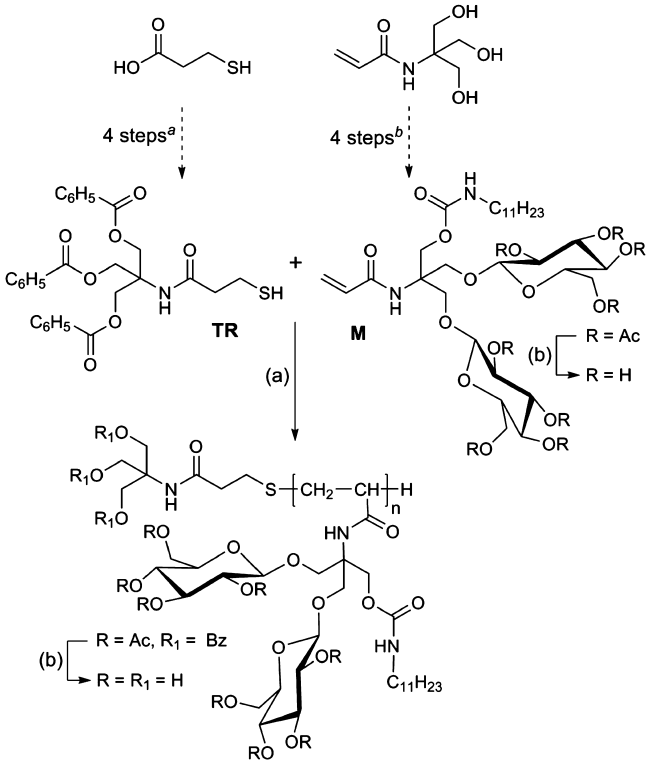

[c][a]Described in ref 15. [b]Described in ref 20. Reagents and conditions: (a) AIBN (0.5 equiv), THF at 66 °C or CH_3CN at 82 °C, argon, 8–24 h, ~30–60%; (b) MeONa, MeOH, pH 8–9, room temperature, argon, 12 h, ~75% for NA$_h$Pols, quantitative yield for deprotected monomer *d***M**.

dx.doi.org/10.1021/la205026r | Langmuir 2012, 28, 4625–4639

$d\mathbf{M}$ were determined using a Zetasizer Nano-S model 1600 (Malvern Instruments Ltd., UK) equipped with a He−Ne laser (λ = 633 nm, 4.0 mW). The time-dependent correlation function of the scattered light intensity was measured at a scattering angle of 173° relative to the laser source. NA_hPol stock solutions were prepared at 100 g·L^{-1} in Milli-Q water and were stored overnight at room temperature. On the day of the experiment the solutions were filtered through a 0.45 μm PVDF syringe filter, diluted to the final concentration, and the size of the particles was measured 1 h after filtration. Other conditions were as reported elsewhere.[21]

Aqueous Size-Exclusion Chromatography (ASEC). NA_hPol stock solutions were prepared at 100 g·L^{-1} in Milli-Q water under magnetic stirring overnight at 4 °C and then diluted 10 times in 100 mM NaCl 20 mM Tris buffer (pH 8). A 100 μL of the latter solution was injected onto a Superose 12 10−300GL column (bed volume: 20 mL; void volume: 7.5 mL; separation range: D_H = 2−18 nm) connected to a Äkta purifier 10 system (GE-Healthcare) and calibrated according to the procedure reported elsewhere.[22] The column was equilibrated with (a) 20 mM Tris/HCl buffer, 100 mM NaCl, pH 8, for analyzing NA_hPols particles and OmpX/A8−35 complexes; (b) 20 mM phosphate buffer, 100 mM NaCl, pH 7, for BR/NA_hPols complexes; and (c) 20 mM phosphate buffer, 100 mM NaCl, pH 6.75, for OmpX/NA_hPols complexes.

Experiments were run at room temperature. The flow rate was set at 0.5 mL·min^{-1} and elution profiles followed at 220, 280, and/or 554 nm.

Buffers in Density, AUC, and SANS Measurements. Buffer H: 100 mM NaCl, 20 mM NaH_2PO_4/Na_2HPO_4, pH 7.4 in Milli-Q water. Buffer D: 100 mM NaCl, 20 mM NaH_2PO_4/Na_2HPO_4 in >99% ^{2}H atom sterile filtered D_2O (Spectra Gases, Inc.). The pH was 7.4 for the analysis with NA29 and 6.8 for the analysis with NA11. Buffer H and Buffer D for NA11 contained in addition 0.02% NaN_3.

NA_hPols Sample Preparation for Density, AUC, and SANS Measurements. NA_hPols were placed at 4 °C in the dark and under vacuum in a desiccator and were dried over phosphorus pentoxide for two months. Solutions at 5, 10, and 15 g·L^{-1} were prepared in H_2O or D_2O by precise weighing of the powder, solvents, and solutions. Complementary experiments were done, in Buffer H and Buffer D, with NA29 at 5 g·L^{-1} and NA11 at 5−15 g·L^{-1}.

Determination of the Partial Specific Volume from Density Measurements. Those were performed using a density-meter DMA5000 (Anton PAAR, Graz Austria). Partial specific volume, $\bar{v}$, was obtained from solvent and solution densities, ρ° and ρ (g.mL^{-1}), measured at concentration c (g.mL^{-1}) according to

$$(\rho - \rho^\circ) = (1 - \rho^\circ\bar{v})/c \tag{4}$$

Analytical Ultracentrifugation. Sedimentation velocity experiments were performed using a Beckman XL-I analytical ultracentrifuge and an AN-50 TI rotor (Beckman Coulter, Palo Alto CA USA). The experiments were carried out at 20 °C and at 42 000 rpm, with cells with double sector centerpiece of 1.2 or 0.3 cm optical path (l), filled typically with ∼420 or 100 μL of sample and of reference solvent. Scans were recorded every ∼5 or 10 min, overnight, using interference optics, and, for the protein samples, at 280 nm, and for BR analysis 555 nm. The sedimentation profiles were analyzed by the size-distribution analysis of Sedfit (free available at http://www.analyticalultracentrifugation.com). In Sedfit, finite element solutions of the Lamm equation for a large number of discrete, independent species, for which a relationship between mass, sedimentation, and diffusion coefficients, s and D, is assumed, are combined with a maximum entropy regularisation to represent a continuous size-distribution.[23] The linear fit $s/s_0 = (1 - k_s c)$ provided an estimate of the sedimentation, s_0, at infinite dilution, and the concentration dependency factor, k_s. The s-value depends in the ideal case on the mass, M, and hydrodynamic diameter, D_H, of the particle, and on the solvent density, ρ, and viscosity, η, according to the Svedberg equation

$$s = M(1 - \rho\bar{v})/(N_A 3\pi\eta D_H) \tag{5}$$

In deuterated solvent, Svedberg equation is slightly modified in view of the increase of mass of the particle—from M to M_D—related to H-D exchange

$$s = M(M_D/M - \rho\bar{v})/(N_A 3\pi\eta D_H) \tag{6}$$

These two equations were used to calculate s_{20w} from the experimental values of s. The frictional ratio f/f_{min} relates D_H and the diameter of the anhydrous particle volume D_{min}

$$D_H = f/f_{min} D_{min} \tag{7}$$

Fringes displacement J characterizing the boundary is related to the refractive index increments $\partial n/\partial c$ (mL/g) and species concentration c (g.mL^{-1}), with λ the wavelength of the laser (675×10^{-7} cm in our experiments), according to

$$(\partial n/\partial c) = (J/c)(\lambda/l) \tag{8}$$

For the study of the complexes, the protein concentration was derived from the absorbance signal at 280 nm, and the amount of bound NA_hPol from the combination of fringe shift and absorbance signals. The derived composition was used for the calculation of the partial specific volume of the complex for the calculation of s_{20w} and f/f_{min}.

As numerical values, for the $c(s)$ analysis, we typically used 200 generated sets of data on a grid of 300 radial points, calculated using frictional ratio of typically 1.2 sometimes fitted, and a regularization procedure with a confidence level of 0.68, and considered $\bar{v}$ determined by density and $\bar{v}$ = 0.76 mL.g^{-1} for the samples of NA_hPol and complexes, respectively. We measured for H_2O, D_2O, and hydrogenated and deuterated buffer densities of 0.9982, 1.1053, 1.0052, and 1.1116 g.mL^{-1} and viscosities of 1.002, 1.295, 1.079, and 1.299 mPa.s, using a density-meter DMA 5000 and viscosity-meter AMVn (Anton PAAR, Graz Austria). M_D/M = 1.015 was estimated for NA29 in 100% D_2O, considering 10 exchangeable H per monomer in addition to 4 others for the whole polymer, thus 424 exchangeable H for a macromolecule of 28 899 Da. Numerical values for BR are given in ref 24. Numerical values used for dOmpX are as follows: molar mass of the monomer in Buffer H: 17 161 g·mol^{-1}; M_D/M = 1.012 corresponding to 80% of exchanged exchangeable hydrogens; $\bar{v}$ = 0.68 mL.g^{-1}; $(\partial n/\partial c)$ = 0.187 mL.g^{-1}; molar extinction coefficient at 280 nm: 31 860 M^{-1}·cm^{-1}.

SANS Experiments and Raw Data Reduction. NA_hPols samples and the respective buffers (all ∼160 μL) were prepared at several H_2O/D_2O ratios (0%, 30%, 70%, and 100% D_2O for NA11 at 15 g·L^{-1}; 0%, 10%, 20%, 30%, 60%, 70%, 80%, and 100% D_2O for NA29 at 15 g·L^{-1}, and at 5 and 10 g·L^{-1} at 0% and 100% D_2O, respectively). The BR/NA29 complexes were measured at three different protein concentrations: 8.85, 4.42, and 2.20 g·L^{-1} (in Buffer H), and 9.70, 4.80, and 2.40 g·L^{-1} (in Buffer D). Measurements were done at 20 °C on the instrument D22 at the Institute Laue-Langevin (ILL) (Grenoble, France) in Hellma quartz cuvettes 100QS with 1 mm optical path length. Scattering data were recorded with a wavelength of λ = 6 Å at an instrumental collimator/detector configuration of 2 m/2 m (NA29 and complexes) and of 1.4 m/1.4 m and 5.6 m/5.6 m (NA11). At each configuration, the H_2O/D_2O-buffers, the empty beam, an empty quartz cuvette, and a boron sample (electronic background) were measured. Exposure times varied from 30 min to 2 h for individual samples, transmission measurements about 3 min. The raw data were reduced with a standard *ILL* software package.[25] The corrected scattered intensities $I(Q)$ (with the scattering vector $Q = (4\pi/\lambda)\sin\theta$, where 2θ is the scattering angle) from different Q-ranges were merged and the buffer signals subtracted using the program "PRIMUS".[26]

SANS Data Analysis. The radii of gyration, R_g, and the intensities in the forward scattering direction, $I(0)$, of all samples were extracted by the Guinier approximation, in the valid range of $R_gQ \leq 1.3$[27]

$$\ln[I(Q)] = \ln[I(0)] - 1/3R_g^2Q^2 \tag{9}$$

dx.doi.org/10.1021/la205026r | *Langmuir* 2012, 28, 4625−4639

The masses of NA_hPols particles, M, were determined from the $I(0)$ intensities in 100% H_2O and 100% D_2O according to[28]

$$M = \frac{1 - T_W}{f 4\pi T_S} \frac{I(0)}{I_{inc}(0)} \frac{N_A 10^3}{Ct} [b - \rho_N{}^0 \bar{v}]^{-2} \quad (10)$$

$I_{inc}(0)$ and $T_W = 0.523$ are the incoherent scattering in the forward direction and the neutron transmission rate of 1 mm optical path water, respectively, T_S is the neutron transmission rate of the sample, C the NA_hPol concentration in mg.mL^{-1}, t = 1 mm is the thickness of the quartz cuvette, f = 0.81 at 6 Å is a correction factor for the anisotropicity of the solvent scattering, ρ_N^0 is the solvent neutron scattering length density in cm^{-2}, and b is the scattering length density of the polymer, in cm/g. We used $\rho_N^0 = -5.62 \times 10^9/6.40 \times 10^{10}$ cm^{-2} for H_2O and Buffer H/D_2O and Buffer D; $b = 8.84 \times 10^9/1.79 \times 10^{10}$ cm/g in H_2O/D_2O, for NA_hPol from the chemical composition of NA29 (see above) and considering a full exchange. For NA29, $I(0)$ at infinite dilution was extrapolated from the linear regression of $C/I(0)$ versus C.[29] The contrast match points were determined experimentally by the intersection of a linear fit through all points with the abscissa of $(I(0)/[T_S C])^{1/2}$ as a function of D_2O content. The pair distance distribution function, $p(r)$, was determined for NA29 at 15 g·L^{-1} in 100% H_2O and 100% D_2O using the program GNOM in user default mode.[30] For an ideal particle of volume V, $p(r) = 4\pi r^2 V\gamma(r)$, with $\gamma(r)$ the autocorrelation function defined as the average of the product of the two scattering density contrasts (cm^{-2}) separated by a distance r.

The final 1D SANS curves corresponding to the BR/NA29 complexes alone (without contribution from free micelles) were obtained in two steps: (1) extrapolation of the scattering curves in both Buffer H and Buffer D at infinite dilution using the concentration series and the protocol developed by Costenaro et al.[29] (2) Subtraction of the free NA_hPol contribution from their extrapolated curves in H_2O and D_2O, respectively. Analysis of the forward intensities was made according to ref 24. The $p(r)$ from the BR monomer (PDB entry 1QHJ) was obtained with GNOM from its back-calculated scattering curve using the program CRYSOL.[31] Those corresponding to the BR/NA29 complexes were extracted with GNOM from the reduced scattering curves (as described above). The low-resolution model of the BR/NA29 complex was obtained using the program DAMMIF[32] from the complex data in Buffer D. DAMMIF uses a single phase with homogeneous contrast to the solvent to model a low-resolution shape. We chose Buffer D rather than Buffer H since in the former the contrast of all components (BR, NAPol, and lipids) was highest and most homogeneous. The shape therefore represents an approximation of a slightly heterogeneous system. It reflects the global shape of the complex and the structural details must not be overinterpreted. The high-resolution monomer was superposed by hand into the overall density.

Protein Purification. *Bacteriorhodopsin.* *H. salinarum* cells (S9 strain, a gift of G. Zaccaï, IBS Grenoble) were grown under light at 37 °C in a liquid growth medium containing 12 g·L^{-1} peptone (LP0037, Oxoïd) as described in ref 33. Purple membrane (PM) was isolated as described in ref 34 and stored at −80 °C. Further steps were performed at 4 °C in the dark. PM containing BR at 6 g·L^{-1}, suspended in 20 mM sodium phosphate buffer, pH 7.0, was solubilized by incubation during 40 h at 4 °C in the dark with 100 mM octylthioglucoside (OTG; cmc ∼9 mM). After centrifugation for 20 min at 200 000 × g in the TLA 100.2 rotor of a TL 100 ultracentrifuge (Beckman Coulter France), the supernatant was diluted to 18 mM OTG with detergent-free buffer. Aliquots of NA_hPols stock solutions (100 g·L^{-1} in water) were added to 250 μL samples to reach final protein/polymer mass ratios of 1:5 or 1:10.

OmpX. Overexpression of uniformly ^2H,^{13}C, and ^{15}N-labeled OmpX (hereafter, dOmpX, labeled in view of its use for NMR experiments) was prepared as described in ref 7. Briefly, the protein was expressed in *E. coli* and purified from inclusion bodies using procedures similar to those described in refs 35 and 36. Inclusion bodies were solubilized in 6 M urea, 20 mM Tris-HCl, 5 mM EDTA, pH 8.5. OmpX was refolded by slow dilution into a solution of dihexanoylphosphatidylcholine (DHPC, Avanti Polar Lipids) at 4 °C. The final protein concentration was 0.46 g·L^{-1} in 2% (w/v) DHPC.

Preparation of Amphipol/Membrane Protein Complexes. *Bacteriorhodopsin.* Final proteins preparations were incubated 15−20 min at 4 °C with aliquots of NA_hPols or A8−35 stock solutions (100 g·L^{-1} in water) to reach the final protein/polymer mass ratio (1:5 or 1:10 w/w for ASEC analysis, 1:5 w/w for AUC and SANS experiments). The detergent was removed by incubation with polystyrene beads (Bio-Beads SM2, 10 g per g detergent) for 2 h under gentle stirring on a wheel. After elimination of the beads and a 20 min centrifugation at 100 000 × g in the TLA 100.2 rotor of a TL 100 ultracentrifuge (Beckman Coulter France), the protein concentrations were determined spectroscopically. For AUC and SANS measurements on BR/NA29 complexes, a 40 mL sample at 0.25 g·L^{-1} BR was concentrated using 4 mL centrifugal filter Amicon Ultra 30 000 MWCO (Millipore) and by running several centrifugations in Buffer H to a final volume of 1 mL at ∼9 g·L^{-1} BR. 500 μL of this final sample was used for SANS and AUC experiments. The remaining 500 μL was diluted eight times in Buffer D and centrifuged (5 min at 3000 × g) in Amicon Ultra filter tubes (Beckman rotor JA-25.50). The procedure was repeated twice. The final sample (500 μL of BR/NA29 at ∼10 g·L^{-1} in Buffer D) was used for SANS and AUC experiments. AUC experiments were performed with diluted samples (5 and 15 μL of each sample diluted to 120 μL in the appropriate buffer). SANS experiments were performed without dilution and with samples diluted 2/3 and 1/3 from the stock solutions. The samples at 30% D_2O was prepared from Buffer D and the stock samples in Buffer H.

OmpX. OmpX trapping by NAPols was performed as reported for trapping the transmembrane domain of outer membrane protein A[37] with A8−35, i.e., at a 1:4 OmpX/NAPol ratio (w/w). DHPC was removed with BioBeads: after 30 min incubation in the presence of NAPols, the beads were added at a 10:1 bead/detergent mass ratio. Beads were removed by centrifugation after 3 h of incubation at room temperature. In order to remove any residual traces of DHPC, 10 cycles of dilution/concentration were performed using a centrifugal filter unit (10 kDa cutoff, Amicon, Millipore) with the NMR buffer: 20 mM phosphate buffer, 100 mM NaCl, 0.05% NaN_3 (pH 6.8) in 10% D_2O. The final sample contained ∼1.3 mM dOmpX.

RESULTS

Synthesis of NA_hPols. The synthesis of NA_hPols is based on three key steps: (i) synthesis of the thiol-based transfer reagent (**TR**),[15] (ii) synthesis of the diglucosylated amphiphilic protected monomer (*p***M**),[20] and (iii) free-radical homotelomerization (Scheme 2). The synthesis of the transfer reagent (**TR**) was performed as previously described,[15] starting from 3-mercaptopropionic acid. Briefly, the thiol function was protected by a trityl group, followed by condensation of *tris*-(hydroxymethyl)-amidomethane (Tris) onto the carboxylic acid group. The three hydroxyl groups of Tris were next protected by benzoyl groups and the trityl protective group was finally removed to lead, after purification, to the transfer reagent in ∼40% overall yield, in four steps. Thanks to the aromatic groups grafted onto Tris, determination of the molecular mass of the final polymers can be achieved by UV and ^1H NMR measurements. The key molecule of NA_hPol preparation is the di-*O*-acetylated glucose-based THAM monomer *p***M** endowed with an undecyl chain, which was synthesized as recently reported.[20] First, two hydroxyl groups of THAM were protected by reaction with dimethoxypropane. The remaining hydroxyl group was then hydrophobized by reaction with undecylisocyanate in basic conditions. Subsequent removal of the 1,3-dioxane protective group followed by diglucosylation

dx.doi.org/10.1021/la205026r | Langmuir 2012, 28, 4625−4639

using tetra-*O*-acetylated glucopyranosyl bromide led to monomer *p*M in ~40% overall yield in four steps.

Free radical homo-telomerization of **M** was performed either in refluxing THF or in refluxing acetonitrile in the presence of **TR** as transfer reagent and azobisisobutyronitrile (AIBN) (0.5 equiv/[**TR**]) as an initiator. The reaction was monitored by thin layer chromatography and carried on until full disappearance of the monomer spot. The number-average degree of polymerization ($\overline{DP}_n$) was set by the initial ratio of **M** to **TR** (R_0), considering, in a first approximation, the transfer constant of **TR** to **M** (C_t) to be close to 1.[38] Surprisingly, important deviations of $\overline{DP}_n$ from R_0 were observed when the reaction was performed in acetonitrile (Table 1). Whereas the R_0 for batch NA10 was set to 50, the resulting polymer exhibited a $\overline{DP}_n$ of ~15. A similar observation was made with batch NA8, for which the R_0 was set to 60 and the resulting $\overline{DP}_n$ was only ~10. Under such conditions, complete consumption of monomer was never observed and the reaction was stopped after ~18 h. On the contrary, in refluxing THF, the $\overline{DP}_n$ was always close to the initial ratio (Table 1). This suggests that in THF C_t is close to 1, as usually observed during homo-telomerization of THAM monomers,[15,16] while it is not in acetonitrile. Gromov and colleagues have demonstrated that for hydrophobic acrylamide-based monomers, the highest rate of polymerization was reached in the less polar mixed-solvent system. Such an effect may be due to hydrophobic associations of polymer chains and the formation of microdomains, which in turn could lead to a micellar catalysis of the reaction.[39] Considering the lower polarity of THF (ε = 7.6) compared to that of acetonitrile (ε = 37.5), the formation of hydrophobic domain during the polymerization of the protected monomer *p*M in refluxing THF is therefore more likely. This may lead to higher rate of polymerization allowing a complete consumption of *p*M within 18 h of reaction despite its bulkiness. On the contrary, in the very polar acetonitrile the micellar catalysis is not favored leading to very low rate of polymerization. The batch-to-batch reproducibility in THF was good, with similar overall yields and a comparable molecular weight of the resulting polymers. Acetylated NA_hPols were purified by preparative size exclusion chromatography (SEC) in organic solvents on hydroxylpropylated cross-linked dextran. The purified acetylated polymers were readily soluble in usual organic solvents such as methanol, chloroform, and toluene, as well as in DMF or DMSO. Simultaneous deprotection of the acetyl and benzoyl groups was achieved under the Zemplén conditions, yielding the amphiphilic polymers (Scheme 2). Pure NA_hPols were obtained in ~50% yield after purification by dialysis against water using cellulose membranes, followed by lyophilization. Throughout the present article, NA_hPols are denoted by a short name reflecting their chemical structure: the letters NA stand for "nonionic amphiphilic homopolymer", followed by the average molecular weight expressed in kDa. Batch numbers are given in Table 1.

Table 1. Synthesis Conditions and Composition of Seven Batches of NA_hPols

					$\bar{M}_n$ of polymers (kDa)[b]		
					Protected NAPols		
NA_hPols	Batch	Solvent[a]	R_0[b]	$\overline{DP}_n$[c,d]	UV[d]	NMR[e]	NA_hPols[f]
NA10	SS 174	ACN	50	15	15	n.d.[g]	10
NA8	SS 293	ACN	60	10	10	n.d.	8
NA45	SS 259	THF	75	66	68	n.d.	45
NA63	SS 292	THF	60	91	94	108	63
NA29	SS 298	THF	40	43	44	50	29.5
NA31	SS 318	THF	40	45	46	n.d.	30.8
NA11	SS 325	THF	15	17	17	18	11.3

[a]Telomerization reactions were carried out either in refluxing acetonitrile (ACN) or in refluxing tetrahydrofuran (THF). [b]Initial molar ratio of protected monomer to transfer reagent. [c]$\overline{DP}_n$ (degree of polymerization) = number of monomer units +1. [d]Determined by UV spectroscopy. [e]Determined by NMR calibration. [f]Calculated from the $\bar{M}_n$ value of the protected polymers determined by UV spectroscopy. [g]n.d.: not determined.

Structure Determination. The $\bar{M}_n$ of the polymers was determined by two methods: (i) by determining the ratio of the mass concentration of acetylated NA_hPol solutions to the molar concentration, determined from the UV absorption (λ_{max} = 272 nm), of the three benzoyl groups grafted at the end of the polymer backbone (Scheme 2); (ii) by comparing the integrated values of the ^{1}H NMR signal of the benzoyl groups to those of the NH vicinal methylene of each amphiphilic monomer constituting the polymer backbone (Figure 1). A good correlation was observed between the two techniques (Table 1), particularly for the shorter polymers. For the protected NA11, for instance, $\bar{M}_n$ values determined by the UV and NMR techniques were 17 and 18 kDa, respectively. For longer polymers, the difference observed between the two spectroscopic techniques was slightly larger but remained <10%, demonstrating the suitability of the two approaches. Values obtained by SEC in DMF using polystyrene standards for the protected and deprotected forms of NA11 were ~4−5× lower

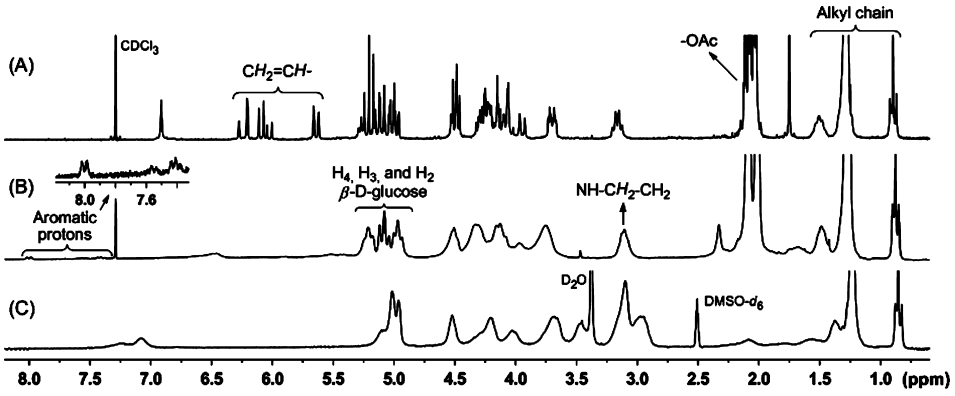

Figure 1. ^{1}H NMR spectrum of (A) Protected monomer *p*M in $CDCl_3$; (B) protected NA29 in $CDCl_3$, and (C) deprotected NA29 in DMSO-d_6.

dx.doi.org/10.1021/la205026r | *Langmuir* 2012, 28, 4625−4639

than the estimates obtained by UV and NMR spectroscopy (data not shown), as previously reported with heteropolymeric NAPols.[15] This factor was similar for both protected and deprotected forms of NA11, suggesting that these inconsistencies are due to the inadequacy of calibrating SEC columns using polystyrene polymers. Hereafter, we therefore rely only on those estimates obtained by the two spectroscopic approaches.

Physical-Chemical Investigation. *Surface Tension Activity.* The surface activity of NA_hPols at the air/water interface was determined by the Wilhelmy plate technique at 25 °C. Figure 2 shows the evolution as a function of concentration of

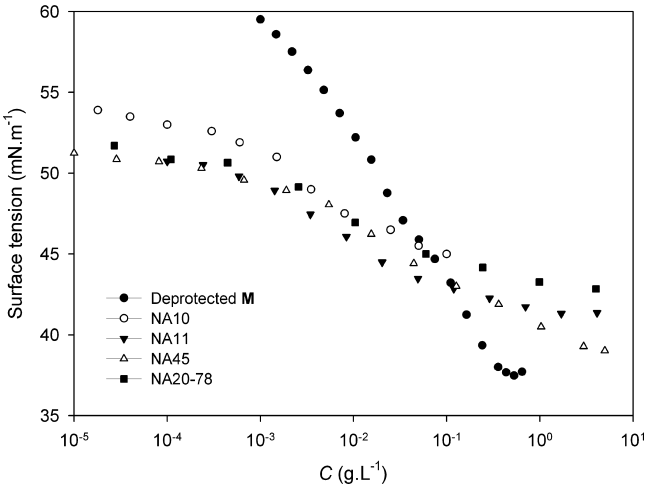

Figure 2. Evolution of the surface tension of aqueous solutions of NA_hPols, a heteropolymeric NAPol (NA20−78; see ref 15) and the deprotected monomer (*d***M**) as a function of concentration. Measurements were done at 22 ± 1 °C.

the surface tension of aqueous solutions of NA10, NA11, and NA45. At variance with detergent solutions, whose surface tension ceases to drop once the cmc is reached and the chemical potential of the solute stabilizes, the surface tension vs concentration plot of NA_hPols does not show any clear break at any concentration, but a monotonous decrease, which is slightly more pronounced with larger polymers (by 12 $mN \cdot m^{-1}$ from 0.01 $mg \cdot L^{-1}$ to 5 $g \cdot L^{-1}$ for NA45). For the sake of comparison, the surface tension of solutions of NA20−78, a heteropolymeric NAPol from the first series, is also plotted in Figure 2, showing a very similar behavior. On the contrary, the surface tension activity of the deprotected monomer was that of a classical detergent, with a cmc of 0.44 ± 0.04 $g \cdot L^{-1}$ (0.65 ± 0.06 mM), similar, as expected from the length of the alkyl chain, to that of *n*-undecyl-*β*-D-maltoside (0.59 mM, from Anatrace catalog, http://www.affymetrix.com).

Dynamic Light Scattering. NA_hPols are highly soluble in water. Their solutions are transparent and remain fluid up to a concentration of 100 $g \cdot L^{-1}$, above which their viscosity increases. Dynamic light scattering (DLS) measurements carried out at 10 $g \cdot L^{-1}$ showed NA_hPols to form well-defined particles, ∼6 nm in diameter, with an average polydispersity of ∼1.6 nm, regardless of the length of the polymer (Figure 3 and Table 2). The smallest NA_hPol, NA8, appeared to differ somewhat from the rest of the series, forming slightly smaller particles ($D_H \approx$ 4.5 nm), but this difference was not confirmed by ASEC data (see below, Table 2). Neither phase separation nor important change of particle size was observed from 0.1 to 100 $g \cdot L^{-1}$ and from 2 to 70 °C for NA29, NA10, and NA8 (Figure S1 and

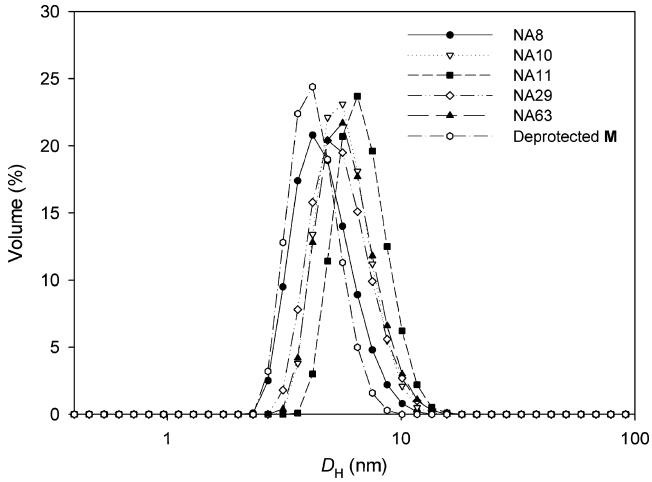

Figure 3. Particle size distribution by volume of NA_hPols (10 $g \cdot L^{-1}$) and of deprotected monomer (5 mM) determined by dynamic light scattering at 20 °C. Data are averages of ten measurements.

Tables S1 and S2). For the sake of comparison, the deprotected monomer was included in the DLS study. Its micelles have a small diameter (∼5.0 nm) and a narrow size distribution (∼1.2 nm) quite similar to those of NA_hPol particles (Figure 3 and Table 2).

Aqueous Size-Exclusion Chromatography (ASEC). Upon ASEC, all NA_hPols appeared to form relatively monodisperse particles (Figure 4). In keeping with DLS data, their average size and dispersity varied very little with the length of the polymer (Table 2). Larger particles, if present at all, are almost undetectable (Figure 4). According to ASEC, the apparent hydrodynamic diameter of NA_hPol particles is ∼6 nm, consistent with that determined by DLS. By ASEC and DLS, NA_hPol particles appeared significantly smaller than those formed by A8−35 (Figure 4). This conclusion, however, is not confirmed by AUC and SANS data since A8−35 particles have a mean molecular mass of ∼40 kDa, thus significantly smaller than that of NA_hPol (see below and ref 9). A8−35 particles are highly charged,[8] while NA_hPol particles are not. Their different elution volumes most likely reflect the existence of different interactions with the chromatographic support. As regards the hydrodynamic diameter of A8−35 particles estimated by DLS, its accuracy is limited, because the samples contained a small amount of large aggregates.[9]

Density Measurements. The density of NA29 in H_2O was determined at 20 °C. Solutions at 0, 4.93, 9.80, and 14.79 $g \cdot L^{-1}$ had densities of 0.99820, 0.99931, 1.00044, and 1.00161 $g \cdot mL^{-1}$, respectively, yielding for the specific volume a value $\bar{v}$ = 0.771 ± 0.002 $mL \cdot g^{-1}$.

Analytical Ultracentrifugation (AUC). Analytical ultracentrifugation allows us to investigate the structural homogeneity of macromolecules in solution as well as characterizing the mass and size of amphiphile self-assemblies (reviewed in refs 40, 41). In keeping with DLS and ASEC data, sedimentation velocity analysis of aqueous solutions of NA29 revealed the presence of very homogeneous particles (Figure 5), with only one major contribution to the $c(s)$ distribution. Larger species in very minor amounts (<2%) may be present in the range 5−15 S, but their presence is difficult to ascertain. The $c(s)$ distributions at 5 and 10 $g \cdot L^{-1}$ in H_2O and at 5, 10, and 16 $g \cdot L^{-1}$ in D_2O showed the same features, indicating that the size of the particles remains the same (data not shown).

dx.doi.org/10.1021/la205026r | *Langmuir* 2012, 28, 4625−4639

Table 2. Physical Characterization of NA$_h$Pols Particles in Aqueous Solution

	DLS[a,b]		ASEC			AUC		Densimetry	SANS	
	D_H[c] (nm)	HHW[d] (nm)	V_e[e] (mL)	HHW[d] (mL)	D_H[f] (nm)	f/f_{min}[g]	s_0[h] (S)	$\bar{v}$[i] (mL·g^{-1})	R_g[j] (nm)	$p(r)_{max}$[k] (nm)
*d***M**	5.0	1.2	-	-	-	-	-	-	-	-
NA10	5.8	1.4	13.4	0.6	5.9	-	-	-	-	-
NA8	4.5	1.3	13.4	0.7	5.9	-	-	-	-	-
NA11	6.4	1.9	13.5	0.5	5.7	1.15 ± 0.05	3.50	-	2.5	6.0
NA29	5.4	1.7	13.5	0.6	5.8	1.15 ± 0.05	3.65	0.771	2.5	6.0
NA63	5.6	1.6	13.4	0.6	5.9	-	-	-	-	-
A8−35	7.2[l]	-	12.5[m]	1.1[m]	6.3[l]; 7.1[m]	-	1.6[l]	0.866[n]	2.4[l]	-

[a][*d***M**] = 5 mM. [b][NAPol] = 10 g·L^{-1}. [c]Hydrodynamic diameter of the particles. Data are the average of ten measurements; standard deviations were <0.2 nm on D_H and <0.1 nm on HHW. [d]HHW, width of the peak at half-height. [e]Elution volume. [f]Hydrodynamic diameter as determined from calibration with soluble proteins. [g]Frictional ratio. [h]Sedimentation coefficient at infinite dilution. [i]Partial specific volume (NAPols) or operational parameter φ' (A8−35). [j]Radius of gyration in H_2O. [k]Maximum particle dimension from $p(r)$ function. [l]From ref 9. [m]This work. [n]φ', from ref 9.

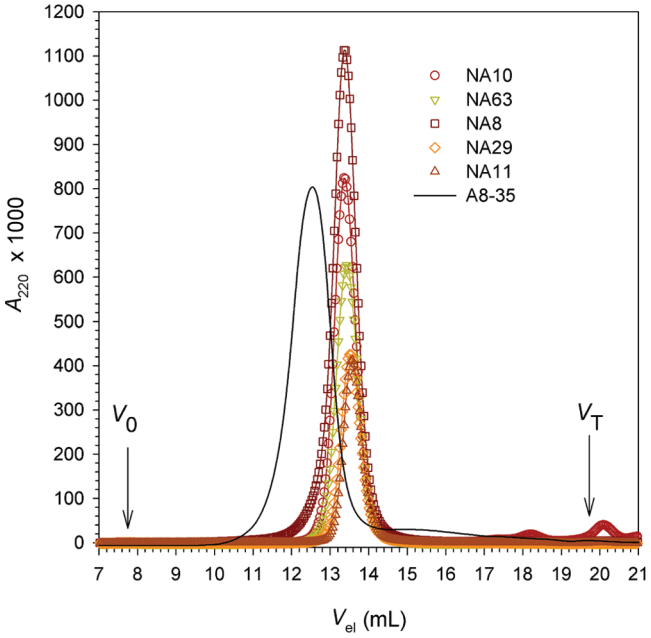

Figure 4. Aqueous size exclusion chromatography elution profiles of NA$_h$Pols and A8−35 at 10 g·L^{-1} in 0.1 M NaCl, 20 mM Tris/HCl buffer, pH 8.0. Detection was done at 220 nm. V_0 (7.9 mL) and V_T (20.1 mL) stand for the exclusion volume and the total volume of the column, respectively.

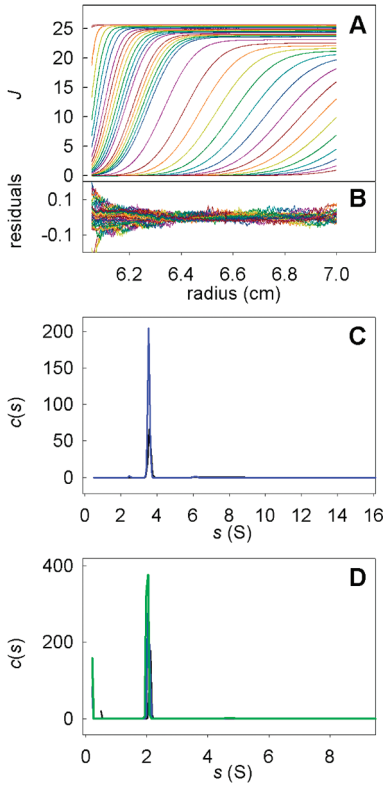

Figure 5. Sedimentation velocity analysis of NA29 in H_2O and D_2O at 42 000 rpm and 20 °C. Detection with interference optics. (A) Superimposition of selected experimental profiles for NA29 in H_2O at 10 g·L^{-1}, corrected for all systematic noises (*dots*), and of the corresponding models (derived from the $c(s)$ analysis; *lines*). The selection includes profiles obtained ca. every 5 min during the first 40 min of centrifugation, then profiles obtained ca. every 25 min up to 8 h of sedimentation. (B) Corresponding residuals. (C) Superimposition of the distributions obtained in H_2O at 9.80 (*blue*) and 4.93 (*black*) g·L^{-1}, showing a main species sedimenting at 3.55 and 3.60 S, respectively. (D) Superimposition of the distributions obtained in D_2O at 16.02 (*green*), 9.82 (*blue*) and 4.92 (*black*) g·L^{-1}, showing a main species sedimenting at 2.01, 2.06, and 2.11 S, respectively.

The slight decrease of the sedimentation coefficient observed upon increasing the concentration is expected from weak excluded volume effects. The related value of the concentration dependency factor, k_s = 4 ± 1 mL·g^{-1}, is identical to that found previously for NA25−78, a heteropolymeric NAPol.[15] The value of the sedimentation coefficient extrapolated at infinite dilution, s_0, is 3.65 S in H_2O and 2.1 S in D_2O, the lower value in D_2O reflecting the higher density and viscosity of the solvent. The linear dependency of the number of fringes of the boundaries vs NA29 concentration (not shown) provides an estimate of the refractive index increment $(\partial n/\partial c)_\mu$ = 0.149 ± 0.004 mL·g^{-1}, a parameter of use for the analysis of MP/NA$_h$Pols complexes. The combination of s_0 in H_2O with the D_H values in the range 5.4−6.0 nm obtained from DLS and ASEC provides a mass for the NA29 particles of 52 ± 3 kDa. The derived value from s_0 in D_2O is very similar: 56 ± 3 kDa. Thus, NA29 particles very likely comprise on average 2 molecules with an average number of alkyl chain of ∼75 (Table 3). This suggests that the longest polymers will combine with the shortest ones so that the number of alkyl chain remains roughly constant. From the estimation of particle masses, the frictional ratio was found to be in the range 1.1−1.2, indicating a

dx.doi.org/10.1021/la205026r | *Langmuir* 2012, 28, 4625−4639

Table 3. Composition and Properties of NAPols and NAPol Particles

amphipols		$\overline{DP_n}$	$\overline{M}_n$ (kDa)	mean number of alkyl chains per molecule	particle mass (kDa) AUC	particle mass (kDa) SANS	mean number of molecules per particle	mean number of alkyl chains per particle
1st series[a]	NA 20−78	51	20	∼11	53	-	∼2.7	∼29
2nd series[b]	NA 25−75b	64	25	∼16	75	-	∼3.0	∼47
	NA 12.5−75	32	12.5	∼9	76	-	∼6.1	∼53
3rd series[c]	NA29	43	29.5	∼42	52 ± 3[d]	47 ± 4[e]	∼1.8	∼75
	NA11	17	11.3	∼16	52 ± 3[d]	50 ± 1[e]	∼4.6	∼74

[a]Data from ref 15. 1st-series NAPols were obtained by co-telomerization of a hydrophilic and an amphiphilic monomer and therefore are referred to as co-telomers. [b]Data from ref 16. 2nd-series NAPols were obtained by homo-telomerization of a single hydrophilic monomer followed by hydrophobization of the resulting polymer and therefore are referred to as grafted homopolymers. [c]This work. 3rd-series NAPols are obtained homo-telomerization of an amphiphilic monomer and therefore are referred to as homopolymers. [d]Molecular weight determined from the combination of the sedimentation coefficient from AUC and a mean value for the hydrodynamic diameter of 5.8 nm. [e]Mean values of the molecular weight obtained in H_2O and D_2O from SANS. Molecular weight was obtained from extrapolation to infinite dilution for NA29, and from measurement at 15 g·L^{-1} for NA11.

compact, globular arrangement. Complementary experiments were done with NA29 and NA11 at 5 g·L^{-1} in phosphate buffers containing 100 mM NaCl, prepared in either H_2O or D_2O (respectively, Buffer H and Buffer D; details in Materials and Methods). All samples contained homogeneous particles, with sedimentation coefficients of 3.4 and 3.5 S in Buffer H and 2.0 and 2.2 S in Buffer D, respectively. These values are very close to those determined for NA29 in pure H_2O and D_2O, suggesting that the particles formed by the two polymers are similar and essentially insensitive to the presence of 100 mM salt.

Small-Angle Neutron Scattering. The neutron scattering curve of NA29 is that expected from compact, globular particles, whose shape does not vary in the concentration range 5−15 g·L^{-1} whether in H_2O or in D_2O (data not shown). In H_2O, the radius of gyration (R_g) was found to be 2.54 ± 0.06 nm, whatever the concentration. In D_2O, R_g appeared to decrease very slightly upon increasing the concentration, from 2.01 ± 0.01 nm at 5 g·L^{-1} to 1.93 ± 0.01 nm at 15 g·L^{-1}. Normalized forward intensities also slightly decreased with the concentration, in logical relation with nonideal excluded volume effects. The extrapolated values at infinite dilution yielded particle masses of 50 ± 1 kDa both in H_2O and in D_2O, in excellent agreement with the results from AUC. The SANS curves of NA11 measured at 15 g·L^{-1} in phosphate buffer presented the same features, with derived radii of gyration of 2.52 ± 0.09 nm and 1.90 ± 0.01 nm and masses of 44 and 51 kDa in buffers containing 100% H_2O and 100% D_2O, respectively. In keeping with DLS, ASEC, and AUC data, the overall dimensions and masses of NA11 and NA29 particles are thus indistinguishable, despite the different average length of the two polymers.

As expected in view of their similar chemical composition, the contrast match points determined for NA29 and NA11 are the same within experimental errors (Figure 6A). The most precisely determined value, 29.9% D_2O for NA29, is very close to that expected from the chemical composition and partial specific volume (29.5% D_2O).

Figure 6B also shows that the structural similarity between NA11 and NA29 particles goes beyond the information contained in the R_g. Indeed, scattering curves for the two polymers are essentially identical whatever the contrast conditions, the minor differences being likely due to slightly different sample concentrations or solvent compositions. Both the size and the internal structure of NA11 and NA29 particles are thus virtually identical. The drastic changes observed in scattering curves upon varying the percentage of D_2O in the solvent result from the spatial segregation of hydrophilic and hydrophobic polymer moieties, which have very different contrast match points, mainly due to their different hydrogen contents. The differences in the pair distance distributions calculated in H_2O and D_2O for NA29 (Figure 6C) can be logically explained by the presence of a hydrophobic particle core (mainly $-CH_2-$ units, with a contrast match point at ∼10% D_2O) surrounded by a hydrophilic shell (mainly sugar moieties, with a contrast match point at ∼40% D_2O). At 0% D_2O, the outer shell has the highest contrast and the particle appears larger, whereas at 100% D_2O the inner core has the highest contrast and the particle appears smaller: the maximum of the pair distance distribution function is thus shifted from 3.3 nm in H_2O to 2.3 nm in D_2O. This distribution also explains that the radii of gyration of NA11 and NA29 are about 0.5 nm smaller in D_2O than in H_2O. The maximum particle dimension of ∼6.0 nm yielded by the $p(r)$ function (Figure 6C) is consistent with the D_H estimates obtained by DLS and ASEC.

Biochemical Validation. Two criteria qualify a polymer as an APol: keeping MPs soluble in aqueous solutions in the absence of detergents, and doing so thanks to the formation of small complexes in which native MPs are individually trapped.[6] Trapping experiments using two model MPs, bacteriorhodopsin and OmpX, showed that NA$_h$Pols fulfill both criteria.

Trapping Membrane Proteins with NA$_h$Pols. BR is a proton pump from the archaebacterium *H. salinarum*, whose transmembrane domain is folded into seven α-helices.[42] Its cofactor, retinal, is covalently linked via a Schiff base to a lysine residue in the last transmembrane helix. Because the spectrum of retinal is exquisitely sensitive to its environment, the visible spectrum of BR is an excellent reporter of the functional state of the protein. OmpX is an eight-stranded β-barrel that spans the outer membrane of *E. coli*. Its three-dimensional structure has been established by X-ray crystallography[36] and studied by solution NMR both in detergent solution[43,44] and as a complex with APol A8−35.[45,46] Both BR (Figure S2) and OmpX (not shown) were quantitatively retained in solution after supplementing their detergent solutions with A8−35, NA10, NA11, or NA29 and removing the detergent by adsorption onto BioBeads, whereas in the absence of APols the two MPs precipitated upon detergent removal. Similar results were observed with tOmpA, the transmembrane domain of *E. coli*'s outer membrane protein A.[47] BR is in its native state after trapping with NA$_h$Pols: its UV/visible spectrum is identical to that of the native detergent-solubilized or A8−35-trapped protein (Figure S3), and it carries out its entire photocycle.[7]

dx.doi.org/10.1021/la205026r | *Langmuir* 2012, 28, 4625−4639

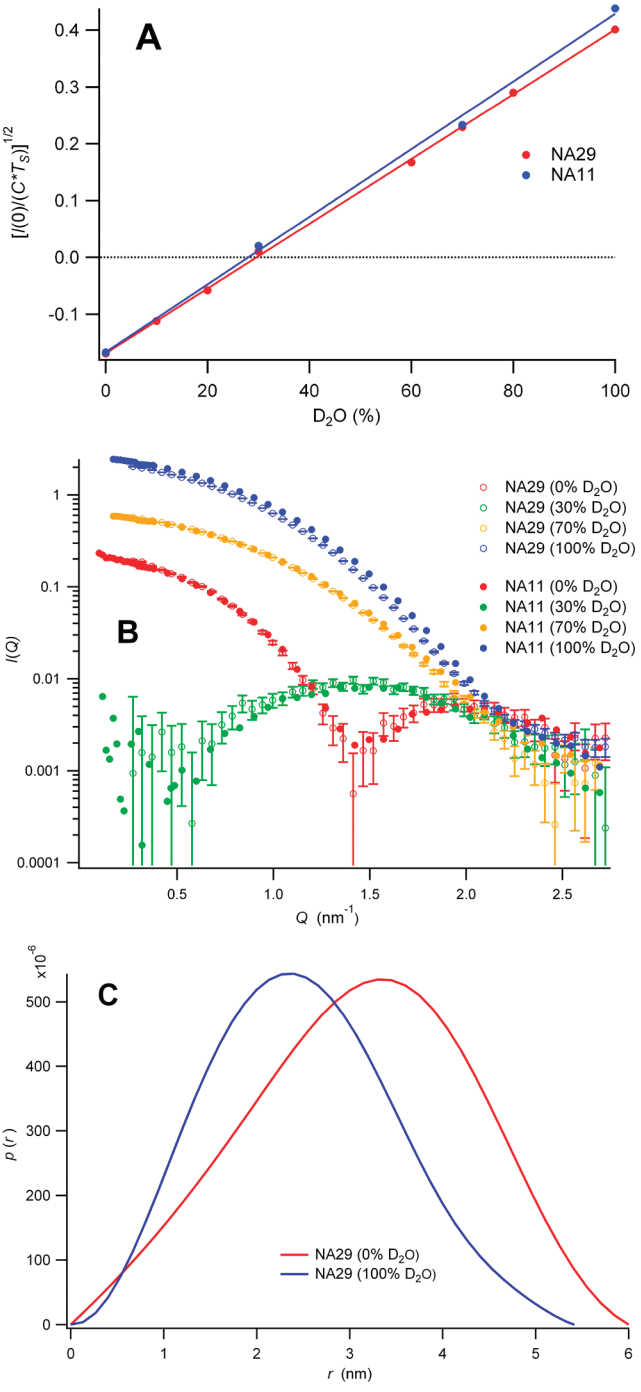

Figure 6. Small angle neutron scattering of NA29 and NA11. (A) Determination of the contrast match points of NA29 (*red*) and NA11 (*blue*) at 15 g·L^{-1}. Derived values are 29.9% and 29.1% D_2O, respectively. (B) Comparison of the scattering curves of NA29 (open symbols) and NA11 (closed symbols) solutions at 15 g·L^{-1} in 0%, 30%, 70%, and 100% D_2O. The error bars on NA29 data are comparable to those on NA11 ones and have been omitted for clarity. (C) Comparison of pair distance distribution functions for NA29 particles at 15 g·L^{-1} in 0% and 100% D_2O.

OmpX, as shown by NMR 2D spectra, retains its native 3D conformation.[7]

Size of Membrane Protein/NA$_h$Pol Complexes As Estimated by ASEC. The size of BR/NA$_h$Pol and OmpX/NA$_h$Pol complexes was studied by ASEC (Figure 7, Figure S4 and ref 47). When trapping was carried out at 1:5 MP/NA$_h$Pol mass

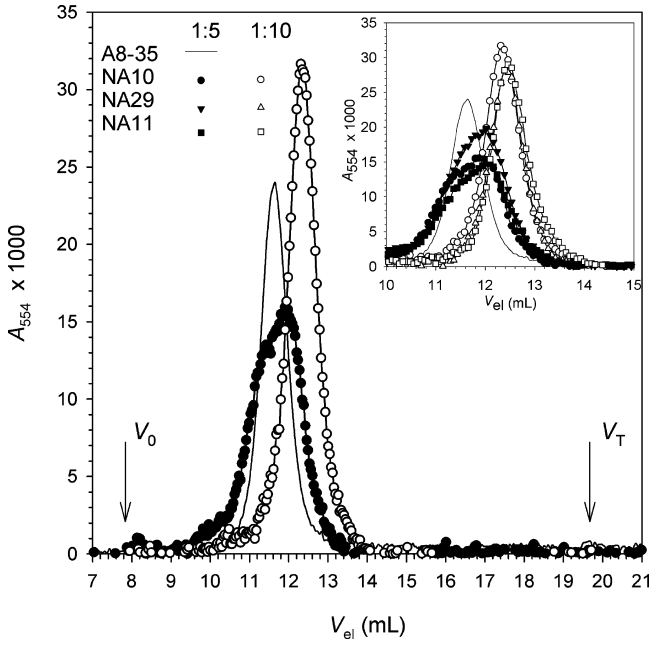

Figure 7. ASEC elution profiles of BR/NA$_h$Pol and BR/A8−35 complexes at 554 nm. For clarity, the profiles for NA$_h$Pol NA10 and A8−35 are shown only for BR/APol = 1:5 w/w. Inset: Enlargement of the elution peaks of the BR/APol complexes for NA10, NA29, NA11, and A8−35, at BR/APol ratios of 1:5 and 1:10 w/w.

ratio, polydisperse complexes were observed, whereas at 1:10 w/w, the complexes appeared essentially monodisperse. This behavior has already been observed when MPs are trapped in the absence of a sufficient excess of A8−35.[48] The apparent sizes of homogeneous BR/NA10, BR/NA11, and BR/NA29 complexes were comparable ($D_H \approx 8.2$ nm). The apparent size of OmpX/NA11 complexes is $D_H \approx 7.2$ nm (Figure S4). Two differences between MP/NA$_h$Pol and MP/A8−35 complexes are to be noted. First, a higher mass ratio of NA$_h$Pol is needed to observe monodisperse complexes by ASEC (~10 g per g BR vs ~4−5 g per g BR for A8−35[24]). Second, as already observed with pure APol particles (Figure 7), BR/NA$_h$Pol complexes elute later from the Sepharose column than BR/A8−35 ones (Figure 7). Whether this corresponds or not to an actual size difference was investigated by AUC and SANS.

Analytical Ultracentrifugation of MP/NA$_h$Pols Complexes. BR/NA29 complexes were subjected to sedimentation velocity analysis at protein concentrations of 1 and 0.3 g·L^{-1}, in hydrogenated and deuterated buffers (Buffer H and Buffer D). Detection was carried out by measuring the absorption at 280 and 555 nm and with interference optics. Figure 8 shows the $c(s)$ distributions obtained for BR at 1 g·L^{-1} in Buffer H and in Buffer D. The samples at 0.3 g·L^{-1} (data not shown) behaved similarly, except that the main peak moved slightly faster than at 1 g·L^{-1} (by 0.2 S), which may be related to excluded volume effects or to uncertainty on the measurements. Free NA$_h$Pol is detected only using interference optics, at 3.7 S in Buffer H and 2.1 S in Buffer D ($s_{20,w}$ = 3.8 S), that is close to the values observed for pure NA$_h$Pols solutions (Table 2). Its concentration was estimated to ~1.1 and ~0.65 g·L^{-1}, respectively. The complex is detected with the three optics, the main peak corresponding to ~90% of the signals in Buffer H and ~95% in Buffer D. Mean s-values were 5.6 ± 0.1 S in Buffer H and 3.2 ± 0.1 S in Buffer D ($s_{20,w}$ = 6.1 S). The ratio A_{280}/A_{555} = 1.6 indicates that BR was in its native,

dx.doi.org/10.1021/la205026r | *Langmuir* 2012, 28, 4625−4639

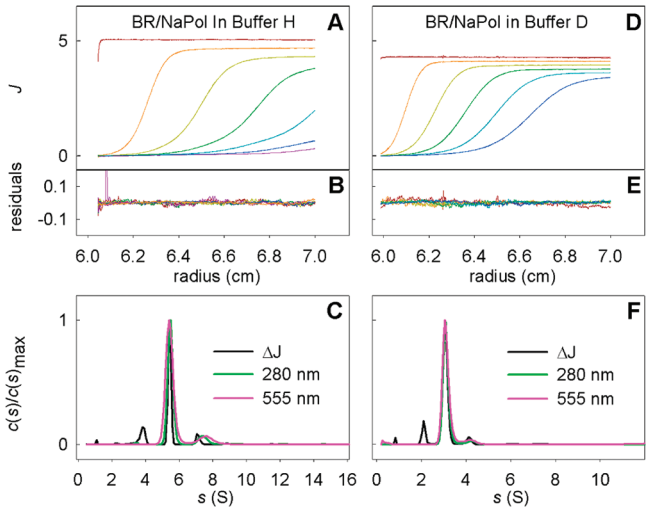

Figure 8. Sedimentation velocity analysis of BR/NA29 complexes at 42 000 rpm and 20 °C. (A) Superimposition of selected experimental profiles for BR/NA29 complexes at 1.17 g·L^{-1} BR in hydrogenated buffer (Buffer H), obtained by interference optics and corrected for all systematic noises (*dots*), and of the corresponding models (derived from the *c*(*s*) analysis; *lines*). 46 profiles collected over 14 h were fitted for the analysis, but the selection includes only seven profiles collected at hourly intervals. (B) Differences between the experimental and modeled profiles. (C) Superimposition of the distributions obtained using interference optics (*black*), and absorbance at 280 nm (*red*) and 555 nm (*blue*). (D–F) Corresponding data for BR/NA29 complexes at 1.06 g·L^{-1} BR in deuterated buffer (Buffer D).

Table 4. Compared Properties of BR/NA29 and BR/A8-35 Complexes

complexes	BR/NA29[a]	BR/A8−35[b]
$s_{20,w}$ (S)[c]	6.1	3.2
A_{280}/A_{555}[d]	1.6	1.6
Bound lipid/BR (g per g BR)[e,f]	n.d.	0.38
Bound APol/BR[g] (g per g BR)[g]	3.6	1.8
D_H (from AUC; nm)[h]	8.2	6.8
D_H (from ASEC; nm)[i]	8.2	10.0
f/f_{min}[j]	1.19	1.10
R_g (nm)[k]	3.5	3.0
$p(r)_{max}$ (nm)[k]	9	n.d.
M_{BR} (Da)[l]	27 067	27 067
M_{lipid} (Da)[f]	10 285	10 285
M_{APol} (Da)	97 441	48 721
$M_{complex}$ (Da)	134 794	86 073
BR-bound APol alkyl chains	∼136	∼110
D_{min} (from composition; nm[m]	7.0	6.2
$\bar{\nu}_{complex}$ (mL·g^{-1})[n]	0.791	0.856

[a]Present work. [b]From ref 24. [c]From AUC; ±0.2 S. [d]From AUC. [e]By chemical analysis. [f]Whenever needed for AUC and SANS calculations, the mass ratio of bound lipids to BR in BR/NAPol complexes was assumed to be identical to that determined in ref 24 for BR/A8−35 ones. [g]From AUC; ±0.2 g/g. [h]From $s_{20,w}$ + composition. [i] ±0.3 or 0.2 nm, respectively. [j]From s_{20w} + composition. In ref 24, a frictional ratio of 1.25 was derived from a consensus R_S of 3.8 nm. [k]From SANS, in hydrogenated buffer. [l]From sequence. [m]Diameter of anhydrous sphere with same composition. [n]from composition, $\varphi'_{complex}$ for BR/A8−35.

retinal-binding state. The signal at 280 nm was used to derive the protein concentration and combined with the interference signal to derive the amount of bound NA$_h$Pol, namely, ∼3.6 g per g BR, assuming the presence of 0.38 g bound lipid per g BR.[24] Assuming BR to be a monomer, the total mass of the complex would be ∼135 kDa (Table 4). The *s*-values and the estimate of bound NA$_h$Pol then indicate that the complexes are rather compact, with a frictional ratio of 1.19 ± 0.02 and a hydrodynamic diameter D_H = 8.2 ± 0.2 nm, the latter value being identical to that determined by ASEC. Minor larger species that moved ∼1.4× faster were also detected. They are most probably complexes comprising two molecules of BR (a dimer moves 1.6× faster than a monomer of the same shape and composition). Additional larger species were possibly present in too minor amounts to be characterized.

Perdeuterated OmpX (dOmpX)/NA11 complexes (prepared in view of NMR studies[7]) were studied by AUC in three buffers with different percentages of D_2O: 0%, 30%, and 100% (Figure S5). As in the case of BR, the behavior of the complexes was similar in the three buffers. Free NA$_h$Pol particles were seen at $s_{20,w}$ = 3.8 S in a proportion of 1.2−1.5 g per g of dOmpX, i.e., ∼0.48−0.60 g·L^{-1} for samples at 0.4 g·L^{-1} dOmpX. The predominant complex, which accounts for >95% of the protein, migrated at $s_{20,w}$ = 5.4 S. From the combination of the A_{280} and interference signals, the amount of bound NA$_h$Pol could be estimated to 4.1 ± 0.4 g NA11 per g dOmpX. This value increases from 3.7 to 4.5 g/g along with the D_2O content in the solvent, but this variation remains within experimental uncertainties. Considering dOmpX as a monomer, the *s*-values and the estimate of bound NA$_h$Pol are compatible with rather compact complexes, with a frictional ratio of 1.2 ± 0.04 and a hydrodynamic diameter D_H = 7.2 ± 0.4 nm. The hypothesis that the main peak contains dOmpX as a dimer can be rejected, since the shape of the complexes would have to be very elongated (frictional ratio of 1.9) to account for the low value of *s*, with $D_H \approx 14$ nm, a value much larger than the estimate from ASEC (Figure S4) and incompatible with SANS data (not shown). A few percents of OmpX form small aggregates, the most populated ones migrating 1.5× faster than the main complex. The same samples, investigated by SANS, revealed the presence of a small fraction of large aggregates (data not shown). Those were seen neither in ASEC nor in AUC analyses (Figures S4 and S5), presumably because these techniques are much less sensitive than SANS to the presence of low concentrations of very large particles. In addition, very large species would have been spun down before the AUC analysis started.

SANS Studies of BR/NA$_h$Pol Complexes. BR/NA29 samples analyzed by AUC were collected and subjected to SANS studies. The comparison of experimental data collected at BR concentrations of ∼10, ∼5, and ∼2.5 g·L^{-1} revealed significant interparticle effects at all concentrations (data not shown). These are logically related to the crowding of the samples, which contain complexes whose mass is ∼5× that of BR, with, in addition, free NA$_h$Pol particles at concentrations similar to that of BR (see above). Figure 9A shows the SANS curves corresponding to the BR/NA$_h$Pols complexes in Buffer H and Buffer D, after subtraction of the contributions from free NA$_h$Pol and extrapolation of the experimental data at infinite dilution. Guinier plots of the two curves are shown in the inset. The Guinier fits are of high quality and indicate radii of gyration of 3.47 ± 0.10 and 3.02 ± 0.06 nm in Buffer H and Buffer D, respectively. The decrease by ∼0.5 nm in Buffer D vs Buffer H is similar to that observed for NA$_h$Pol particles in both solvents, as expected from its dominant contribution in the complex. It is consistent with the APol being localized at the periphery of the protein, with its hydrophilic moieties at the

dx.doi.org/10.1021/la205026r | *Langmuir* 2012, 28, 4625−4639

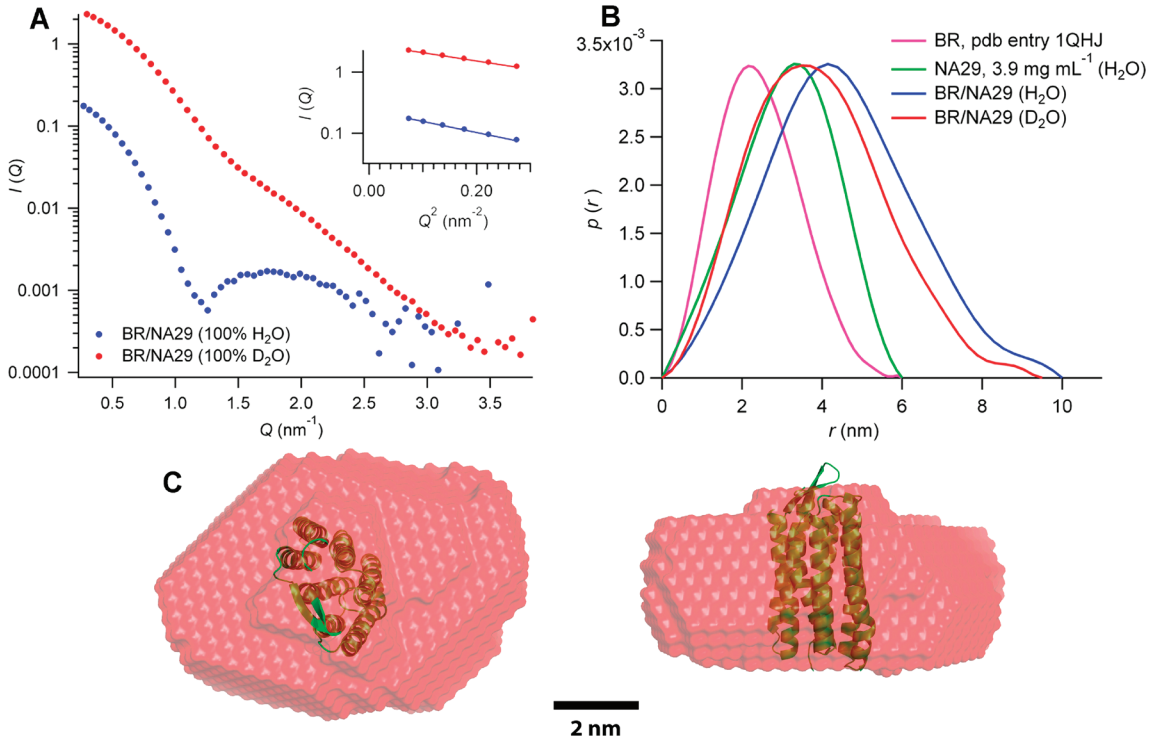

Figure 9. Small angle scattering analysis of BR/NA$_h$Pol complexes. (A) SANS signal corresponding to the BR/NA$_h$Pol complex in hydrogenated buffer (Buffer H) or in deuterated buffer (Buffer D), prepared with either H_2O (*blue*) or D_2O (*red*). The data sets were obtained by extrapolating I/C to infinite dilution and subtracting the signal from the free NA$_h$Pol particles in a weighted manner. The inset shows Guinier plots of the two curves. (B) Pair distance distribution functions (normalized) for the BR monomer (from PDB entry 1QHJ; *purple*), free NA29 particles in H_2O (*green*), and for the BR/NA29 complexes in either H_2O (*blue*) or D_2O (*red*) buffer. (C) Side and top view of the low-resolution envelope for BR/NA29 complexes in D_2O calculated using the program DAMMIF in slow mode. Superposed is the BR monomer (PDB entry 1QHJ).

interface with water, as for the free particle. Experimental forward intensities were compared to those calculated considering the chemical composition of the particles as derived from AUC. Considering a homogeneous complex, expected forward intensities in Buffer H and Buffer D are 3% and 17%, respectively, below experimental values, thus of the right order of magnitude. Taking into account the presence of 10% and 5% dimers in Buffer H and Buffer D, respectively, as suggested by AUC, calculated values diverge by +7% and −13% from the experimental ones. SANS data thus are consistent with the presence of homogeneous or nearly homogeneous BR/NA$_h$Pol complexes.

The $p(r)$ functions calculated for the BR monomer from crystallogaphic data and the experimental $p(r)$ function determined by SANS for free NA$_h$Pol particles have about the same maximum extension (6.0 nm), but the peak of the function is shifted to larger distances for the particles, indicating a more globular shape (Figure 9B). The experimental maximum dimension, D_{max}, of the BR/NA$_h$Pol complex is of the order of 9 nm (Figure 9B), in fair agreement with the hydrodynamic diameter estimated by AUC and ASEC (8.2 ± 0.3 nm; Table 4). A low-resolution envelope was calculated from the SANS data. It displays a globular but slightly oblate form. The short axis has approximately the same length as the transmembrane part of BR, suggesting a possible orientation of BR within the envelope, as shown in Figure 9C. The total volume of the envelope (168 000 Å^3) shows that the volume of the two surfactants (lipid + NA$_h$Pol) is 4.5× that of the monomer BR (30 700 Å^3), which is close to the volume ratio of 4.2 (0.5 from lipid and 3.7 from NA$_h$Pol) calculated from the composition inferred from AUC.

DISCUSSION

Homopolymeric NAPols (NA$_h$Pols) present two advantages over previous NAPols:[15,16] first, the use of a single, amphiphilic monomer whose synthesis is relatively simple helps preparing multigram-scale polymer batches, as required by biological applications; second, because NA$_h$Pols are homopolymers, no batch-to-batch variation can arise from a nonrandom distribution of the alkyl chains, as was the case for earlier NAPols. By varying the monomer/transfer reagent ratio (R_0), NA$_h$Pols of different masses (8−63 kDa) could be obtained. The nature of the reaction solvent turned out to be of high importance to properly control the $\overline{DP}_n$: when telomerization was carried out in refluxing THF, the $\overline{DP}_n$ was always close to the initial monomer/transfer reagent ratio, whereas large discrepancies were observed when using acetonitrile as a solvent. The average chain length of each batch of NA$_h$Pols was established through chain end calibration techniques, using both UV and NMR spectroscopy. A very good correlation between the two methods was observed, $\overline{M}_n$ values differing by no more than 10%.

NA$_h$Pols are highly soluble in water (>100 g·L^{-1}). In aqueous solution, they assemble into small, compact, globular particles, whose size, as determined by AUC and SANS, is comparable to that of the particles formed by A8−35,[9] by SAPols,[13] and by heteropolymeric NAPols.[15,16] The hydrodynamic diameter of NA$_h$Pols particles is ∼6 nm, whatever the length of the chain ($\overline{DP}_n$ = 10−91), which is similar to the size of the micelles formed by the deprotected monomer (Table 2). As regards surface activity, the deprotected monomer behaves like a classical detergent, with a cmc of 0.65 ± 0.06 mM. NA$_h$Pols significantly

dx.doi.org/10.1021/la205026r | *Langmuir* 2012, 28, 4625−4639

reduce the surface tension of water even at low concentration (0.01 mg·L^{-1}), but their surface tension vs concentration curves do not show any clear break. This behavior is identical to that of heteropolymeric NAPols.[15]

The chain length of NA$_h$Pols has no or very little influence on the mass of particles formed in aqueous solutions, ∼50 kDa, which is slightly higher than that of A8−35 particles (∼40 kDa).[9] This corresponds to ∼75 undecyl chains in the hydrophobic core of NA$_h$Pol particles vs ∼80 octyl chains in that of A8−35 particles.[9] Heteropolymeric NAPols have smaller cores (30−50 chains; Table 3; see refs 15, 16), which may be due to a looser packing of their hydrophilic moieties.

The present study shows that NA$_h$Pols qualify as APols, inasmuch as they are able to maintain soluble in detergent-free solutions two test MPs, BR and OmpX, under the form of small, nearly monodisperse complexes, with hydrodynamic radii of 4.1 and 3.6 nm, respectively (Table 4 and Figure S4). There is an apparent discrepancy between analyses by AUC and ASEC of preparations of BR trapped at a 1:5 protein/NA$_h$Pol mass ratio: the complexes appear essentially homogeneous in AUC, but heterogeneous upon ASEC. This difference in behavior is probably related to the fact that ASEC separates free NA$_h$Pol from BR/NA$_h$Pol complexes, while AUC analyzes the migration of the complex at nearly constant concentration of free NA$_h$Pol particles. This observation appears to corroborate the fact that forming homogeneous solutions of MP/APol complexes requires the presence of a small excess of polymer, as noted in earlier studies.[24,48]

Extensive ASEC, AUC, and SANS studies have shown that most BR/A8−35 complexes contain a single copy of BR, along with bound lipids.[24] Similarly, solution NMR data collected on OmpX/A8−35 complexes are consistent with each particle containing a single copy of the protein.[45,46] The same conclusion holds for BR/NA$_h$Pol and OmpX/NA$_h$Pol complexes. Table 4 shows a comparison between the hydrodynamic and scattering properties of the two types of BR complexes. In both cases, SANS, AUC, and ASEC data indicate that the complexes are close to homogeneous, but contain a small percentage of dimers or higher association states. According to AUC and SANS measurements, the size of BR/NA29 complexes is slightly larger than that of BR/A8−35 ones, whereas ASEC measurements tend to overestimate the size of BR/A8−35 complexes, which appear, mistakenly, to be bigger than BR/NA$_h$Pol ones. The most striking difference between BR/NA29 and BR/A8−35 complexes is the amount of bound APol, which is twice as large for NA29 as for A8−35. Despite this large difference in MP/APol mass ratio, BR/NA29 and BR/A8−35 complexes contain about as many hydrophobic chains (∼136 and ∼110, respectively), and their dimensions are roughly similar: the D_H and R_g values of BR/NA$_h$Pol complexes are only ∼1 and 0.5 nm larger (Table 4) than those of BR/A8−35 ones, an increase that is expected considering their different composition (Table 4). The fact that, under appropriate conditions, MP/NA$_h$Pol complexes are small and well-defined is of great importance for many biological applications, including radiation scattering studies (this work), AUC (this work) solution NMR,[7] and, potentially, crystallization.

Trapping by NA$_h$Pol preserves the structure of both BR and OmpX. This is shown here by the spectrum of BR, which is identical to that of BR in detergent solution or after trapping by A8−35 (Figure S3). We show elsewhere that NA$_h$Pol-trapped BR undergoes its entire photocycle, with characteristics very close to that of the protein inserted in its native purple membrane.[7] BR, which is relatively unstable in detergent solution, is strongly stabilized by transferring it from OTG to NA$_h$Pol.[7] Detailed NMR studies have shown that the structure of OmpX kept soluble either by detergents[44] or by A8−35[45,46] is very close to the crystallographic structure.[36] Comparison of HSQC [^{1}H,^{15}N] two-dimensional NMR spectra of NA$_h$Pol-trapped and A8−35-trapped OmpX shows that they are nearly indistinguishable, indicating that the protein has retained its native state upon transfer to NA$_h$Pol.[7]

CONCLUSION

A novel series of nonionic amphipols for handling membrane proteins in detergent-free aqueous solutions has been synthesized. Incorporating amphiphilicity at the monomer level was achieved by homo-telomerization of an amphiphilic monomer bearing two glucose moieties and an undecyl alkyl chain, thus producing the first homopolymeric APols ever to be developed. Nonionic homopolymeric APols were found to be highly soluble in water and to self-organize, within a large concentration range, into small, globular particles of ∼6 nm diameter with a narrow size distribution. They proved able to trap and stabilize two test membrane proteins, bacteriorhodopsin from *H. salinarum* and OmpX from *E. coli*, under their native form, as well-defined, small globular complexes comprising the protein as a monomer associated to ∼4 g polymer per g of protein. These data suggest that MP/NA$_h$Pol complexes can be put to the same types of applications as MP/A8−35 ones have been, with, for some of them, the advantages associated to a lesser sensitivity to pH and ionic conditions, and for others, those resulting from their absence of charges. Thereby, NAPols ought to facilitate the study and folding of MPs whose stability is improved at low pH or depends on the presence of multivalent cations. Also notable is the fact that the insensitivity of NAPols to acidic conditions extends the range of conditions accessible to NMR studies, which will facilitate, in particular, the observation of amide protons that are freely exposed to the aqueous solution.[7] In addition, NAPols open the way to applications that are out of reach of charged APols, such as MP separation by ion exchange chromatography, isoelectrofocusing (PB & EBD, unpublished data), and MP cell-free synthesis.[6,7]

ASSOCIATED CONTENT

Supporting Information

Particle size distribution by volume of NA$_h$Pols determined by DLS at different concentrations and different temperatures; ability of NA$_h$Pols to keep BR soluble in aqueous solution after detergent removal; UV/visible absorbance spectra of BR after trapping with NA$_h$Pols or A8−35; ASEC elution profiles of NA11 particles and OmpX/NA11 complexes; sedimentation velocity analysis of dOmpX/NA11 complexes. This material is available free of charge via the Internet at http://pubs.acs.org/.

AUTHOR INFORMATION

Corresponding Author

*G.D.: gregory.durand@univ-avignon.fr; C.E.: christine.ebel@ibs.fr; J.-L.P.: jean-luc.popot@ibpc.fr.

Present Address

[¶]Département de Chimie et Faculté de Pharmacie, Université de Montréal, Pavillon J. A. Bombardier, CP 6128 Succursale Centre Ville, Montréal QC H3C 3J7, Canada

Notes

The authors declare the following competing financial interest(s): B.P., J.-L.P., K.S.S., P.B., G.D., and F. Giusti hold a patent on non-ionic amphiphilic homopolymers. Pucci, B., Popot, J.-L., Sharma, K. S., Bazzacco, P., Durand, G., Giusti, F. (2009) Polymères comprenant une majorité de monomères amphiphiles destinés au piégeage et à la manipulation de protéines membranaires. Patent FR 2,952,642.

■ ACKNOWLEDGMENTS

Particular thanks are due to Elodie Point (UMR 7099) for her participation in purifying the membrane proteins used in this work and in trapping and ASEC experiments, to Simon Raynal (Université d'Avignon et des Pays de Vaucluse) for his technical assistance in the purification of NA11, to Phil Callow for his technical help in SANS experiments, and to Aline Le Roy (Institut de Biologie Structurale Jean-Pierre Ebel) for her participation in AUC experiments and analysis. Thanks are due to J.-F. Gohy and J.-M. Schumers (Université Catholique de Louvain – Belgium) for the SEC analysis of the protected and deprotected forms of NA11. We thank the IBS platform of the Partnership for Structural Biology and the Institut de Biologie Structurale in Grenoble (PSB/IBS) for access to AUC and Institute Laue-Langevin for beam time on D22. This work was supported by the CNRS, by the Université Paris-7, by the Commissariat à l'Energie Atomique, by the Université Joseph Fourier – Grenoble 1, by the Université d'Avignon et des Pays de Vaucluse, and by grants from the E.U. (Specific Targeted Research Project LSHGCT-2005-513770 *IMPS: Innovative tools for membrane protein structural proteomics* and FP7 Grant agreement N°2265507 - NMI3) and from the French Ministry of Research (ANR 06-BLAN-0087 "Refolding GPCRs" and PCV07_186241 PROMEMSURFII). KSS was funded by *IMPS*. P.B. was the recipient of a fellowship from the European International Training Network *BioMem*.

■ ABBREVIATIONS

AIBN, α,α'-azobisisobutyronitrile
APol, amphipol
ASEC, aqueous size exclusion chromatography
AUC, analytical ultracentrifugation
BR, bacteriorhodopsin
cmc, critical micellar concentration
C_t, transfer constant
DLS, dynamic light scattering
DMF, dimethylformamide
DMSO, dimethylsulfoxide
$\overline{DP}_n$, number-average degree of polymerization
*d***M**, *N*-1,1-di[(*β*-D-glucopyranosyl)oxymethyl]-1-[(undecylcarbamoyloxymethyl)-methyl)]-acrylamide
*p***M**, *N*-1,1-di[(2′,3′,4′,6′-tetra-*O*-acetyl-*β*-D-glucopyranosyl)-oxymethyl]-1-[(undecylcarbamoyloxymethyl)-methyl)]-acrylamide
M, Mass of NA_hPols particles
MP, membrane protein
$\overline{M}_n$, number-average molecular weight of polymers
MW, molecular weight
NAPol, nonionic amphipol
NA_hPol, nonionic homopolymeric amphipol
OmpX, *Escherichia coli*'s outer membrane protein X
OTG, *n*-octyl-*β*-D-thioglucopyranoside
SANS, small-angle neutron scattering
SAPol, sulfonated amphipol
SEC, size exclusion chromatography
SV, sedimentation velocity
TR, transfer reagent
THAM, *tris*(hydroxymethyl)-acrylamidomethane
THF, tetrahydrofuran
TLC, thin-layer chromatography
tOmpA, transmembrane domain of *Escherichia coli*'s outer membrane protein A
Tris, *tris*(hydroxymeythyl)-aminomethane

■ REFERENCES

(1) le Maire, M.; Champeil, P.; Møller, J. V. Interaction of membrane proteins and lipids with solubilizing detergents. *Biochim. Biophys. Acta* **2000**, *1508*, 86–111.
(2) Gohon, Y.; Popot, J.-L. Membrane protein–surfactant complexes. *Curr. Opin. Colloid Interface Sci.* **2003**, *8*, 15–22.
(3) Breyton, C.; Pucci, B.; Popot, J.-L. In *Heterologous expression of membrane proteins: Methods and protocols*, Mus-Veteau, I., Ed.; The Humana Press: Totowa, New Jersey, 2010; Vol. *601*, pp 219–245.
(4) Popot, J.-L. Amphipols, Nanodiscs, and Fluorinated Surfactants: Three Nonconventional Approaches to Studying Membrane Proteins in Aqueous Solutions. *Annu. Rev. Biochem.* **2010**, *79*, 737–775.
(5) Tribet, C.; Audebert, R.; Popot, J.-L. Amphipols: Polymers that keep membrane proteins soluble in aqueous solutions. *Proc. Natl. Acad. Sci. U.S.A.* **1996**, *93*, 15047–15050.
(6) Popot, J.-L.; Althoff, T.; Bagnard, D.; Banères, J.-L.; Bazzacco, P.; Billon-Denis, E.; Catoire, L. J.; Champeil, P.; Charvolin, D.; Cocco, M. J.; Crémel, G.; Dahmane, T.; de la Maza, L. M.; Ebel, C.; Gabel, F.; Giusti, F.; Gohon, Y.; Goormaghtigh, E.; Guittet, E.; Kleinschmidt, J. H.; Kühlbrandt, W.; Le Bon, C.; Martinez, K. L.; Picard, M.; Pucci, B.; Rappaport, F.; Sachs, J. N.; Tribet, C.; van Heijenoort, C.; Wien, F.; Zito, F.; Zoonens, M. Amphipols From A to Z. *Annu. Rev. Biophys.* **2011**, *40*, 379–408.
(7) Bazzacco, P.; Billon-Denis, E.; Sharma, K. S.; Catoire, L. J.; Mary, S.; Le Bon, C.; Point, E.; Banères, J.-L.; Durand, G.; Zito, F.; Pucci, B.; Popot, J.-L. Non-ionic homopolymeric amphipols: Application to membrane protein folding, cell-free synthesis, and solution NMR. *Biochemistry* **2012**, DOI: http://dx.doi.org/10.1021/bi201862v.
(8) Gohon, Y.; Pavlov, G.; Timmins, P.; Tribet, C.; Popot, J.-L.; Ebel, C. Partial specific volume and solvent interactions of amphipol A8–35. *Anal. Biochem.* **2004**, *334*, 318–334.
(9) Gohon, Y.; Giusti, F.; Prata, C.; Charvolin, D.; Timmins, P.; Ebel, C.; Tribet, C.; Popot, J.-L. Well-Defined Nanoparticles Formed by Hydrophobic Assembly of a Short and Polydisperse Random Terpolymer, Amphipol A8–35. *Langmuir* **2006**, *22*, 1281–1290.
(10) Picard, M.; Dahmane, T.; Garrigos, M.; Gauron, C.; Giusti, F.; le Maire, M.; Popot, J.-L.; Champeil, P. Protective and Inhibitory Effects of Various Types of Amphipols on the Ca^{2+}-ATPase from Sarcoplasmic Reticulum: A Comparative Study. *Biochemistry* **2006**, *45*, 1861–1869.
(11) Nagy, J. K.; Kuhn Hoffmann, A.; Keyes, M. H.; Gray, D. N.; Oxenoid, K.; Sanders, C. R. Use of amphipathic polymers to deliver a membrane protein to lipid bilayers. *FEBS Lett.* **2001**, *501*, 115–120.
(12) Diab, C.; Tribet, C.; Gohon, Y.; Popot, J.-L.; Winnik, F. M. Complexation of integral membrane proteins by phosphorylcholine-based amphipols. *Biochim. Biophys. Acta* **2007**, *1768*, 2737–2747.
(13) Dahmane, T.; Giusti, F.; Catoire, L. J.; Popot, J.-L. Sulfonated amphipols: Synthesis, properties, and applications. *Biopolymers* **2011**, *95*, 811–823.
(14) Prata, C.; Giusti, F.; Gohon, Y.; Pucci, B.; Popot, J.-L.; Tribet, C. Nonionic amphiphilic polymers derived from Tris(hydroxymethyl)-acrylamidomethane keep membrane proteins soluble and native in the absence of detergent. *Biopolymers* **2001**, *56*, 77–84.
(15) Sharma, K. S.; Durand, G.; Giusti, F.; Olivier, B.; Fabiano, A.-S.; Bazzacco, P.; Dahmane, T.; Ebel, C.; Popot, J.-L.; Pucci, B. Glucose-Based Amphiphilic Telomers Designed to Keep Membrane Proteins Soluble in Aqueous Solutions: Synthesis and Physicochemical Characterization. *Langmuir* **2008**, *24*, 13581–13590.

(16) Bazzacco, P.; Sharma, K. S.; Durand, G.; Giusti, F.; Ebel, C.; Popot, J.-L.; Pucci, B. Trapping and Stabilization of Integral Membrane Proteins by Hydrophobically Grafted Glucose-Based Telomers. *Biomacromolecules* **2009**, *10*, 3317−3326.
(17) Basu, S.; Vutukuri, D. R.; Shyamroy, S.; Sandanaraj, B. S.; Thayumanavan, S. Invertible Amphiphilic Homopolymers. *J. Am. Chem. Soc.* **2004**, *126*, 9890−9891.
(18) Kale, T. S.; Klaikherd, A.; Popere, B.; Thayumanavan, S. Supramolecular Assemblies of Amphiphilic Homopolymers. *Langmuir* **2009**, *25*, 9660−9670.
(19) Savariar, E. N.; Aathimanikandan, S. V.; Thayumanavan, S. Supramolecular Assemblies from Amphiphilic Homopolymers: Testing the Scope. *J. Am. Chem. Soc.* **2006**, *128*, 16224−16230.
(20) Sharma, K. S.; Durand, G.; Pucci, B. Synthesis and Determination of Polymerization Rate Constants of Glucose-Based Monomers. *Designed Monom. Polym.* **2011**, *14*, 499−513.
(21) Abla, M.; Durand, G.; Pucci, B. Glucose-Based Surfactants with Hydrogenated, Fluorinated, or Hemifluorinated Tails: Synthesis and Comparative Physical-Chemical Characterization. *J. Org. Chem.* **2008**, *73*, 8142−8153.
(22) Harlan, J. E.; Picot, D.; Loll, P. J.; Garavito, R. M. Calibration of Size-Exclusion Chromatography: Use of a Double Gaussian Distribution Function to Describe Pore. *Anal. Biochem.* **1995**, *224*, 557−563.
(23) Schuck, P. Size-Distribution Analysis of Macromolecules by Sedimentation Velocity Ultracentrifugation and Lamm Equation Modeling. *Biophys. J.* **2000**, *78*, 1606−1619.
(24) Gohon, Y.; Dahmane, T.; Ruigrok, R.; Schuck, P.; Charvolin, D.; Rappaport, F.; Timmins, P.; Engelman, D. M.; Tribet, C.; Popot, J.-L.; Ebel, C. Bacteriorhodopsin/Amphipol Complexes: Structural and Functional Properties. *Biophys. J.* **2008**, *94*, 3523−3537.
(25) Gosh, R. E.; Egelhaaf, S. U.; Rennie, A. R. Institute Laue Langevin internal report 2006, ILL06GH05T 2006.
(26) Konarev, P. V.; Volkov, V. V.; Sokolova, A. V.; Koch, M. H. J.; Svergun, D. I. PRIMUS: a Windows PC-based system for small-angle scattering data analysis. *J. Appl. Crystallogr.* **2003**, *36*, 1277−1282.
(27) Guinier, A. La diffraction des rayons X aux très petits angles; application à l'étude de phénomènes ultramicroscopiques. *Ann. Phys.* **1939**, *12*, 166−237.
(28) Jacrot, B.; Zaccai, G. Determination of molecular weight by neutron scattering. *Biopolymers* **1981**, *20*, 2413−2426.
(29) Costenaro, L.; Zaccai, G.; Ebel, C. Understanding the crystallisation of an acidic protein by dilution in the ternary NaCl−2-methyl-2,4-pentanediol−H2O system. *J. Cryst. Growth* **2001**, *232*, 102−113.
(30) Svergun, D. I. Determination of the regularization parameter in indirect-transform methods using perceptual criteria. *J. Appl. Crystallogr.* **1992**, *25*, 495−503.
(31) Svergun, D. I.; Barberato, C.; Koch, M. H. J. *CRYSOL* - a Program to Evaluate X-ray Solution Scattering of Biological Macromolecules from Atomic Coordinates. *J. Appl. Crystallogr.* **1995**, *28*, 768−773.
(32) Franke, D.; Svergun, D. I. *DAMMIF*, a program for rapid *ab-initio* shape determination in small-angle scattering. *J. Appl. Crystallogr.* **2009**, *42*, 342−346.
(33) Oesterhelt, D.; Stoeckenius, W. Isolation of the cell membrane of *Halobacterium halobium* and its fractionation into red and purple membrane. *Methods Enzymol.* **1974**, *31*, 667−678.
(34) Lobasso, S.; Lopalco, P.; Lattanzio, V. M. Osmotic shock induces the presence of glycocardiolipin in the purple membrane of *Halobacterium salinarum*. *J. Lipid Res.* **2003**, *44*, 2120−2126.
(35) Pautsch, A; Vogt, J; Model, K; Siebold, C; Schulz, G. E. Strategy for membrane protein crystallization exemplified with OmpA and OmpX. *Proteins* **1999**, *34*, 167−172.
(36) Vogt, J.; Schulz, G. E. The structure of the outer membrane protein OmpX from Escherichia coli reveals possible mechanisms of virulence. *Structure* **1999**, *7*, 1301−1309.
(37) Zoonens, M.; Catoire, L. J.; Giusti, F.; Popot, J.-L. NMR study of a membrane protein in detergent-free aqueous solution. *Proc. Natl. Acad. Sci. U.S.A.* **2005**, *102*, 8893−8898.
(38) Starks, C. M. *Free radical telomerization*; Academic Press: New York, 1974.
(39) Baranova, A. I.; Bune, E. V.; Gromov, A. V.; Gromov, V. F. Hydrophobic interactions in the radical polymerization of acrylamide derivatives. *Eur. Polym. J.* **2000**, *36*, 479−483.
(40) le Maire, M.; Arnou, B.; Olesen, C.; Georgin, D.; Ebel, C.; Møller, J. V. Gel chromatography and analytical ultracentrifugation to determine the extent of detergent binding and aggregation, and Stokes radius of membrane proteins using sarcoplasmic reticulum Ca^{2+}−ATPase as an example. *Nat. Protoc.* **2008**, *3*, 1782−1795.
(41) Ebel, C. Sedimentation velocity to characterize surfactants and solubilized membrane proteins. *Methods* **2011**, *54*, 56−66.
(42) Henderson, R.; Baldwin, J. M.; Ceska, T. A.; Zemlin, F.; Beckmann, E.; Downing, K. H. Model for the structure of bacteriorhodopsin based on high-resolution electron cryo-microscopy. *J. Mol. Biol.* **1990**, *213*, 899−929.
(43) Fernández, C.; Adeishvili, K.; Wüthrich, K. Transverse relaxation-optimized NMR spectroscopy with the outer membrane protein OmpX in dihexanoyl phosphatidylcholine micelles. *Proc. Natl. Acad. Sci. U.S.A.* **2001**, *98*, 2358−2363.
(44) Fernández, C.; Hilty, C.; Wider, G.; Guntert, P.; Wüthrich, K. NMR Structure of the Integral Membrane Protein OmpX. *J. Mol. Biol.* **2004**, *336*, 1211−1221.
(45) Catoire, L. J.; Zoonens, M.; van Heijenoort, C.; Giusti, F.; Popot, J.-L.; Guittet, E. Inter- and intramolecular contacts in a membrane protein/surfactant complex observed by heteronuclear dipole-to-dipole cross-relaxation. *J. Magn. Reson.* **2009**, *197*, 91−95.
(46) Catoire, L. J.; Zoonens, M.; van Heijenoort, C.; Giusti, F.; Guittet, E.; Popot, J.-L. Solution NMR mapping of water-accessible residues in the transmembrane β-barrel of OmpX. *Eur. Biophys. J.* **2010**, *39*, 623−630.
(47) Bazzacco, P. Non-ionic amphipols: new tools for in vitro studies of membrane proteins. Validation and development of biochemical and biophysical applications. Thèse de Doctorat, Université Paris-7, Paris, 2009.
(48) Zoonens, M.; Giusti, F.; Zito, F.; Popot, J.-L. Dynamics of Membrane Protein/Amphipol Association Studied by Förster Resonance Energy Transfer: Implications for in Vitro Studies of Amphipol-Stabilized Membrane Proteins. *Biochemistry* **2007**, *46*, 10392−10404.